The effective potential and effective Hamiltonian in quantum statistical mechanics

1995 J. Phys.: Condens. Matter 7 7891

(http://iopscience.iop.org/0953-8984/7/41/003)

J. Phys.: Condens. Matter 7 (1995) 7891–7938. Printed in the UK

REVIEW ARTICLE

The effective potential and effective Hamiltonian in quantum statistical mechanics

Alessandro Cuccoli†‡, Riccardo Giachetti†§, Valerio Tognetti†‡, Ruggero Vaia‖‡ and Paola Verrucchi¶‡

† Dipartimento di Fisica, Università di Firenze, Largo E Fermi 2, I-50125 Firenze, Italy
‡ Istituto Nazionale di Fisica della Materia INFM, Unità di Firenze, Italy
§ Istituto Nazionale di Fisica Nucleare INFN, Sezione di Firenze, Italy
‖ Istituto di Elettronica Quantistica CNR, via Panciatichi 56/30, I-50127 Firenze, Italy
¶ ISIS Facility, Rutherford Appleton Laboratory, Oxfordshire OX11 0QX, UK

Received 3 August 1995

Abstract. An overview on the theoretic formalism and up to date applications in quantum condensed matter physics of the effective potential and effective Hamiltonian methods is given. The main steps of their unified derivation by the so-called *pure quantum self-consistent harmonic approximation* (PQSCHA) are reported and explained. What makes this framework attractive is its easy implementation as well as the great simplification in obtaining results for the statistical mechanics of complicated quantum systems. Indeed, for a given quantum system the PQSCHA yields an effective system, i.e. an effective classical Hamiltonian with dependence on $\hbar$ and β and classical-like expressions for the averages of observables, that has to be studied by classical methods. Anharmonic single-particle systems are analysed in order to get insight into the physical meaning of the PQSCHA, and its extension to the investigation of realistic many-body systems is pursued afterwards. The power of this approach is demonstrated through a collection of applications in different fields, such as soliton theory, rare gas crystals and magnetism. Eventually, the PQSCHA allows us also to approach quantum dynamical properties.

1. Introduction

Microscopic phenomena obey the laws of quantum mechanics and the uncertainty principle is unavoidable each time that the considered actions are of the order of magnitude of the Planck constant [1]. The consequences of this fact are far reaching in the framework of statistical mechanics where, by definition, one tries to reconstruct the macroscopic behaviour of the system starting from elementary interactions of their microscopic constituents. Since the notion of phase space itself is deprived of a real meaning, the statistical averages cannot be computed any more 'in the classical way', namely by integrating dynamical variables over coordinates and momenta with a suitable distribution function: one has coherently to start from the quantum definitions and evaluate the appropriate operator traces [2].

Classical averages, however, are objects usually easier to handle, especially from a numerical point of view. Therefore much effort has been devoted to investigating the possibility of defining some functions with properties similar to those of the phase-space distribution functions and called *quasiprobability distributions*. Although, in a strict sense, these functions cannot be considered probability measures (they lack, e.g., the fundamental property of being positive definite), still they can provide a nontrivial physical insight into the properties of the dynamical system. The mathematical problem of their explicit

0953-8984/95/417891+48$19.50

determination is often reduced to the choice of an appropriate representation for computing the operator traces. We shall be more precise on this in the following. Here we want rather to observe that the classical limiting conditions, obviously required, on the one hand allow for a careful investigation of the relevance of quantum effects, while on the other naturally suggest an approach of the semi-classical type.

This review is devoted to a semi-classical approach leading to an effective potential and to an effective Hamiltonian, which allows us to recover the phase-space formalism. The method was introduced by Feynman [1, 2], improved independently by two of us and Feynman and Kleinert [3, 4, 5, 6], and eventually extended to nonstandard Hamiltonians [7]. Many applications proved the validity of the method. Indeed, reviews devoted to specific subjects of interest have been published [8, 9, 10, 11, 12].

Semi-classical approximations can be obtained in several ways, by developing methods that lead to different final results. Although always exact and coincident in the classical limit, different methods have different conditions of applicability as far as the evaluation of quantum effects is concerned. The Wigner–Kirkwood expansion [13, 14, 15, 16, 17], the Weyl representation [18, 16] and the use of coherent states [19, 20, 21] are well known theoretical devices moving in this stream. Starting from the path-integral approach to the statistical mechanics, the effective potential is based on the fundamental idea derived by the renormalization group theory. It is done by integrating out the quantum fluctuations around the classical trajectory in imaginary time so that one can recover a classical-like configuration integral, where the potential contains some renormalized constants. Although exact in principle, the calculation can be performed only at some level of approximation, using some perturbation scheme. The choice of the unperturbed system plays a crucial role for a successful application.

In the Lagrangian form a temperature dependent effective potential was firstly introduced by Feynman [1, 2]. Using an inequality based on the convexity of real exponential functions (the Peierls–Jensen–Feynman inequality [22]) and free particles as a unperturbed systems, a variational procedure was carried out on a single parameter, depending on the average point of the path. This function represents the effective external potential seen by the particle in that point. At highest temperatures the Wigner expansion and eventually the classical potential are recovered, while the approximation is not sufficient to account for the low-temperature behaviour of solid state systems, which are better described by a set of harmonic oscillators rather than free particles.

In order to overcome these difficulties, the method was later on improved so as to take exactly into account the contribution of quadratic terms [3, 4, 5]. In this case, the frequencies of the harmonic modes become themselves variational parameters and it is indeed possible to define an effective potential that reproduces the correct behaviour of the quantum harmonic oscillators at the lowest temperatures. The presence of two variational parameters plays a crucial role in contrast with other attempts on this subject [23, 24].

Starting from the application to one particle [4, 25, 26, 27, 28, 29, 30, 31, 32, 33, 34, 35], two-body systems [36] and transition rate theory [37, 38, 39] this method has been successfully used mostly for investigating nonlinear one-dimensional fields [6, 40, 41, 42, 43, 44, 45, 46, 47] as well as condensed matter systems [48, 49, 50, 51, 52, 53, 54, 55, 56].

The variational inequality, however, turns out to be proved only for Hamiltonians containing a kinetic term quadratic in the momenta with constant coefficients and a potential energy depending only upon the coordinates. We shall refer to these as to *standard* Hamiltonians. Recently, the approach was revisited by several people, in order to overcome the one-loop approximation [35, 57, 58], for treating the anharmonicity of the ground state [59] and for casting the calculations in the usual diagrammatic form [60, 61], by an expansion

based on the 'Feynman centroid density'.

The generalization to many degrees of freedom is not at all straightforward. A further approximation, called the 'low coupling approximation' (LCA), is required [3, 4, 62, 63] in order to do explicit calculations, even though some improvements beyond the LCA have been suggested [56].

The appealing idea of including in the unperturbed system as much as we are able to deal with in an exact way can undergo some generalizations. It is worthwhile to notice that attempts have been made of summing on a finite number of Matsubara frequencies [64, 65] and, more recently, new Trotter number extrapolations in path-integral Monte Carlo (PIMC) find their origin in the effective potential framework [66, 53, 67].

In many cases of physical interest the Hamiltonians are not standard, as occurs, for instance, in the study of magnetic systems. The phase space of spin variables, indeed, has a geometrical structure in which a global distinction of coordinates and momenta is impossible, so that, in principle, the equations of motion can be given only in a canonical formulation. For general Hamiltonian systems the Euclidean action is no longer real and the Peierls–Jensen–Feynman inequality cannot be proven for the reference systems [68] which are in general nonlocal, because they are dependent on the average point of the path. However, the general idea to integrate out the quantum contribution is still appealing and the method was generalized taking into account that, at least for a one-loop approximation, the quantum behaviour can be separated from the classical one, so that the Gaussian approximation can be used only for the purely quantum fluctuations while the classical effects are treated exactly by well established (and much easier) approaches. This scheme, which we introduced for the first time [7], is the application of the 'self-consistent harmonic approximation' to the quantum effects only. All the aforementioned results for the effective potential of standard Hamiltonians are recovered and an effective Hamiltonian can be also obtained in the general case [69, 70]. The latter derivation requires the use of the Hamiltonian path integral with some rules about the ordering procedure; it is indeed well known that different quantum systems have the same classical limit. However, this approach presents not only a broader applicability, but it seems more meaningful and powerful for future applications to field theory.

It is just with this more recent point of view that we derive the effective potential and the effective Hamiltonian for evaluating equilibrium averages of quantum quantities. Starting with one degree of freedom, we parallel the 'self-consistent harmonic approximation' (SCHA) to present the so called 'pure quantum self-consistent harmonic approximation' (PQSCHA), by which we recover the variational effective potential as a particular case.

Some relevant applications, for *nonstandard* systems like magnetic ones [71, 72, 73, 74, 75, 76], showing the validity of the method for the thermodynamics of non linear condensed matter systems, are presented through this review.

The last part of the paper is devoted to the challenging problem of calculating the quantum dynamic correlation functions at finite temperatures. We remember that these quantities are directly related to the spectral shape as probed, for instance, by neutron scattering. It is well known that field theories at finite temperature are crucial in condensed matter physics, but present many difficulties from both the analytical and the numerical point of view. Since any static correlation can be calculated by these methods [77, 6, 60, 78, 79], we have calculated the quantum dynamic correlators improving the behaviour of the naive moment expansion in the time domain [78, 80, 81, 82], by the continued fraction representation of its Laplace transform according to Mori and Dupuis [83, 84, 85]. Finally, a generalization of the explicit expression obtained for the quantum averages has been proposed [86, 61] for calculating averages of operators at different imaginary times,

thus permitting an analytic continuation [87, 88, 89]. From this observation, and from the assumption that the classical motion could be separated from the quantum Gaussian fluctuations, at some level of approximation, the possibility of extending the molecular dynamics to some quantum systems has been recently suggested [90, 91].

2. Standard systems—one degree of freedom

In this section we will derive the *pure quantum self-consistent harmonic approximation* (PQSCHA) [7, 69] in its simplest version, namely the one suitable for studying a single one-dimensional nonrelativistic particle of mass m, with canonical coordinate- and momentum operators $\hat{q}$ and $\hat{p}$ such that $[\hat{q}, \hat{p}] = i\hbar$, and subjected to a potential $V(\hat{q})$. This system is described by the standard Hamiltonian

$$\hat{\mathcal{H}} = \frac{1}{2m}\hat{p}^2 + V(\hat{q}). \tag{2.1}$$

After a brief description of the harmonic (HA) [92, 93] and self-consistent harmonic (SCHA) [94, 95, 96, 97] approximations, both in the classical and in the quantum case, it will be clear to the reader how the effective potential method arises updating the main ideas underlying those simpler approximations by means of the new ideas and mathematical tools introduced by the path-integral formulation of quantum statistical mechanics.

2.1. Harmonic approximations

2.1.1. Classical case. Let us consider a classical system in thermal equilibrium at temperature $T = \beta^{-1}$: its thermodynamic behaviour is completely determined once the (unnormalized) canonical distribution function $\rho(p, q) = \exp[-\beta\mathcal{H}(p, q)]$ is known. The thermal average of any physical quantity $\mathcal{O}(p, q)$ is indeed given by the phase space integral

$$\langle \mathcal{O}(p,q) \rangle = \frac{1}{\mathcal{Z}} \int \frac{dp\, dq}{2\pi\hbar}\, \mathcal{O}(p,q)\rho(p,q) \tag{2.2}$$

where $\mathcal{Z} \equiv \exp(-\beta F)$ is the partition function and F the free energy of the system. In the standard case, if we restrict our interest to those observables $\mathcal{O}(q)$ depending just on q, the kinetic contribution can be integrated out and equation (2.2) takes the form

$$\langle \mathcal{O}(q) \rangle = \frac{1}{\mathcal{Z}} \sqrt{\frac{m}{2\pi\hbar^2\beta}} \int dq\, \mathcal{O}(q)\, e^{-\beta V(q)}. \tag{2.3}$$

The recipe for a harmonic approximation is given by the introduction of a quadratic trial potential

$$V_0(q) = w + \tfrac{1}{2}m\omega^2(q - q_0)^2 \tag{2.4}$$

whose parameters w, ω and q_0 have to be determined according to some optimization criterion; the thermal average is then approximated in terms of a Gaussian distribution

$$\langle \mathcal{O}(q) \rangle \simeq \langle \mathcal{O}(q) \rangle_0 = \frac{1}{\sqrt{2\pi\alpha_C}} \int dq\, \mathcal{O}(q)\, e^{-(q-q_0)^2/2\alpha_C} \tag{2.5}$$

where

$$\alpha_C = \alpha_C(\omega) = \frac{1}{m\beta\omega^2} \tag{2.6}$$

represents the thermally induced mean square fluctuations of q around q_0. The simplest way to determine the parameters is to require that the true and trial potentials, as well as their first and second derivatives, take the same value in q_0,

$$\begin{aligned} &V(q_0) = V_0(q_0) = w \\ &V'(q_0) = V_0'(q_0) = 0 \\ &V''(q_0) = V_0''(q_0) = m\omega^2. \end{aligned} \tag{2.7}$$

This criterion defines the usual HA, in which anharmonic effects are completely neglected: what is done is in fact nothing but the second-order expansion of $V(q)$ around its minimum. It can be easily realized that this approximation worsens when the temperature is raised, since configurations far from the minimum become more and more likely.

One can go beyond the HA by requiring that $V_0(q)$ at best approximates $V(q)$ in the whole thermally relevant region rather than in its minimum: this would mean generalizing conditions (2.7) as $\langle V_0(q)\rangle = \langle V(q)\rangle$ etc, but, since the exact probability distribution is supposed to be unknown, one resorts to the trial Gaussian one, writing

$$\begin{aligned} &\langle V(q)\rangle_0 = \langle V_0(q)\rangle_0 = w + \tfrac{1}{2}m\omega^2\alpha_C \\ &\langle V'(q)\rangle_0 = \langle V_0'(q)\rangle_0 = 0 \\ &\langle V''(q)\rangle_0 = \langle V_0''(q)\rangle_0 = m\omega^2. \end{aligned} \tag{2.8}$$

These equations define the SCHA, the self-consistency being due to the ω-dependence of α_C, i.e. of $\langle\cdots\rangle_0$.

It is easy to check that a variational approach based on the inequality

$$F \leqslant F_0 + \langle V - V_0\rangle_0 \tag{2.9}$$

which is a straightforward consequence of the Jensen one [98], gives exactly the same result, in that conditions (2.8) minimize the right-hand side of this inequality.

In the zero-temperature limit $\alpha_C \to 0$ and the distribution $\langle\cdots\rangle_0$ becomes a delta function; therefore conditions (2.8) become identical to (2.7) and the simple HA is recovered.

2.1.2. Quantum case. Facing the quantum problem, we have now to deal with the (unnormalized) density operator $\hat\rho = \exp(-\beta\hat{\mathcal{H}})$ and with statistical averages

$$\langle\hat{\mathcal{O}}\rangle = \frac{1}{\mathcal{Z}}\operatorname{Tr}(\hat\rho\,\hat{\mathcal{O}}) \tag{2.10}$$

where $\mathcal{Z} \equiv \exp(-\beta F) = \operatorname{Tr}\hat\rho$ and $\hat{\mathcal{O}}$ is an observable. As in the previous subsection, we consider the case of $\hat{\mathcal{O}}$ depending just on the coordinate, so that $\hat{\mathcal{O}} = \mathcal{O}(\hat q)$, although, at variance with the classical context, the extension to the general case is not trivial at all (see section 3.3).

A harmonic approximation with the trial potential $V_0(\hat q)$, equation (2.4), again reduces the average (2.10) to the Gaussian form

$$\langle\mathcal{O}(\hat q)\rangle \simeq \langle\mathcal{O}(\hat q)\rangle_0 = \frac{1}{\sqrt{2\pi\alpha_Q}}\int \mathrm{d}q\, \mathrm{e}^{-(q-q_0)^2/2\alpha_Q}\,\mathcal{O}(q) \tag{2.11}$$

where now

$$\alpha_Q = \alpha_Q(\omega) = \frac{\hbar}{2m\omega}\coth\frac{\beta\hbar\omega}{2} \tag{2.12}$$

is the mean square fluctuation of a quantum harmonic oscillator (see appendix A). As in the classical case, conditions (2.7) and (2.8) determine the value of the parameters appearing in the quadratic trial potential and then define the quantum HA and SCHA, respectively.

A variational approach which turns out to give the same results as the SCHA is still possible, thanks to the Bogoliubov inequality [2]

$$F \leqslant F_0 + \langle \hat{\mathcal{H}} - \hat{\mathcal{H}}_0 \rangle_0. \tag{2.13}$$

In the zero-temperature limit the quantum SCHA remains different from the HA, since the distribution does not reduce to a delta function, as $\alpha_Q \to \hbar/(2m\omega) > 0$ due to the zero-point fluctuations.

Example. Let us consider the anharmonic potential ($m = 1$, $\hbar = 1$)

$$V(q) = \tfrac{1}{2}\omega_0^2 q^2 + \lambda q^4. \tag{2.14}$$

The HA, through equations (2.4) and (2.7), simply gives $q_0 = 0$, $w = 0$ and $\omega^2 = \omega_0^2$. On the other hand, the SCHA, through equations (2.8), gives $q_0 = 0$ and

$$w = -3\lambda\alpha_{C,Q}^2(\omega) \qquad \omega^2 = \omega_0^2 + 12\lambda\alpha_{C,Q}(\omega). \tag{2.15}$$

The last equation has to be solved self-consistently together with the definition of $\alpha_C = (\beta\omega^2)^{-1}$, in the classical case, or $\alpha_Q = \coth(\beta\omega/2)/2\omega$, in the quantum one. In the former case the solution is $\omega^2 = \omega_0^2 + \sqrt{\omega_0^4 + 48\lambda T}$, whereas it can be found numerically (e.g., by iteration) in the second one. Of course, the solution is temperature dependent, and it is seen that the nonlinear part of the potential is partly taken into account as both ω and w depend on λ.

In figure 1 we report the exact quantum density $P(q) = \langle \delta(q - \hat{q}) \rangle$ numerically obtained for this example, compared with its approximations by HA and SCHA, as well as with the classical result for an intermediate temperature $T = 0.3$ in natural units. It appears that the classical density is not yet a good approximation as it indeed becomes at higher T, whereas the HA overestimates the width of fluctuations due to the strong nonlinearity. Eventually, the SCHA turns out to be superior, in spite of its constraint to be a Gaussian.

As we have seen above, a harmonic approximation leads to a Gaussian configuration density, the difference between the classical and the quantum case being in the actual value of the variance (α_C or α_Q). Since the variances of a Gaussian are additive under convolution, we can rewrite equation (2.11) separating the classical thermal fluctuations α_C:

$$\langle \mathcal{O}(\hat{q}) \rangle \simeq \frac{1}{\sqrt{2\pi\alpha_C}} \int \mathrm{d}q \left(\frac{1}{\sqrt{2\pi\alpha}} \int \mathrm{d}\xi\, \mathcal{O}(q+\xi)\, \mathrm{e}^{-\xi^2/2\alpha} \right) \mathrm{e}^{-(q-q_0)^2/2\alpha_C} \tag{2.16}$$

where $\alpha = \alpha_Q - \alpha_C$ can be naturally thought of as the purely quantum contribution to the fluctuations of the particle. Equation (2.16) can be interpreted as the classical average of the Gaussian broadening of $\mathcal{O}(q)$ on the scale of the pure quantum fluctuations. Now, in view of the existence of plenty of theoretical and numerical methods for calculating classical averages, one could speculate whether it is really necessary to retain the HA in the outer classical average, or it could be possible to restore the full classical Boltzmann factor. This idea is suggestive, because in this way one would build up an improved theory describing exactly the effects of nonlinearity at the classical level, as well as the full quantum harmonic behaviour. However, a firmer mathematical basis is in order, and the tool to accomplish this goal is Feynman's path-integral formulation of quantum statistical mechanics.

2.2. *Feynman does it better!*

The (diagonal) density matrix elements in the coordinate representation are expressed by Feynman's path integral as

$$\rho(q) \equiv \langle q|\hat{\rho}|q \rangle = \int_q^q \mathcal{D}[q(u)]\, \mathrm{e}^{\mathcal{S}[q(u)]} \tag{2.17}$$

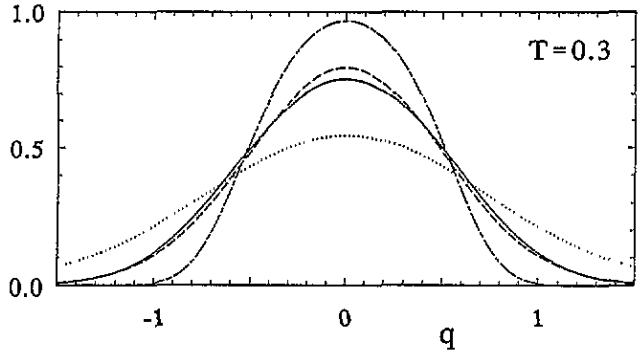

Figure 1. Normalized configuration probability distribution $P(q) = \langle \delta(q - \hat{q}) \rangle$ for the quartic oscillator (2.14) with $\omega_0 = 1$, $\lambda = 1$, at $T = 0.3$. Solid line: exact quantum result; dashed: quantum SCHA; dotted. quantum HA; dash–dotted: classical.

where the path integration is defined as a sum over all paths $q(u)$ closed on q ($q(0) = q(\beta\hbar) = q$) and the Euclidean action

$$S[q(u)] = -\frac{1}{\hbar}\int_0^{\beta\hbar} \mathrm{d}u \left[\frac{m}{2}\dot{q}^2(u) + V\big(q(u)\big)\right] \tag{2.18}$$

has been introduced.

Although the exact evaluation of this integral is possible just in a few cases for simple potentials, the expression (2.17) makes possible a new kind of approximation through a simple and nice idea due to Feynman. The argument proceeds as follows: instead of summing over all paths in just one step, one can classify the paths by an equivalence relation, and consequently decompose the integral into a first sum over all paths belonging to the same class, and a second one over the equivalence classes.

If the equivalence relation among paths is, as Feynman suggested, that of having the same *average point*, defined as the functional

$$\frac{1}{\beta\hbar}\int_0^{\beta\hbar} \mathrm{d}u\, q(u) \tag{2.19}$$

then each class is labelled by a real number $\bar{q}$ representing the common average point, and we can separate from equation (2.17) an ordinary integral over $\bar{q}$,

$$\rho(q) = \int \mathrm{d}\bar{q}\ \bar{\rho}(q;\bar{q}). \tag{2.20}$$

The *reduced* density $\bar{\rho}(q;\bar{q})$ represents the contribution that comes from all those paths with $\bar{q}$ as average point; its explicit expression is therefore

$$\bar{\rho}(q;\bar{q}) \equiv \int_q^q \mathcal{D}[q(u)]\ \delta\left(\bar{q} - \frac{1}{\beta\hbar}\int_0^{\beta\hbar} \mathrm{d}u\, q(u)\right)\ \mathrm{e}^{S[q(u)]}. \tag{2.21}$$

Let us now consider $\bar{\rho}(q;\bar{q})$ as an unnormalized probability in the variable q and define its normalization constant as $\rho_{\mathrm{eff}}(\bar{q})$, so that $\bar{\rho}(q;\bar{q}) = \rho_{\mathrm{eff}}(\bar{q})\,\mathcal{P}(q;\bar{q})$. Then the average of $\mathcal{O}(\hat{q})$ can be written using (2.21) as

$$\langle \mathcal{O}(\hat{q}) \rangle = \frac{1}{\mathcal{Z}}\int \mathrm{d}q\ \mathcal{O}(q)\rho(q) = \frac{1}{\mathcal{Z}}\int \mathrm{d}\bar{q}\left(\int \mathrm{d}q\ \mathcal{O}(q)\mathcal{P}(q;\bar{q})\right)\rho_{\mathrm{eff}}(\bar{q}) \tag{2.22}$$

and one recognizes $\rho_{\mathrm{eff}}(\bar{q})$ as a classical-like effective density, whereas the probability distribution $\mathcal{P}(q;\bar{q})$ concerns the particle fluctuations around the point $\bar{q}$. In the classical

limit it can be seen that $\mathcal{P} \to \delta(q-\bar{q})$ and $\rho_{\rm eff}(\bar{q})$ tends to the classical Boltzmann factor; it follows that the probability $\mathcal{P}$ describes the pure quantum fluctuations of the particle. In other words, we have made an exact formal separation between a classical-like and a pure quantum contribution to $\langle\mathcal{O}(\hat{q})\rangle$.

The main problem is now the explicit evaluation of the reduced density $\bar{\rho}(q;\bar{q})$, still containing a path integral: it is here that some kind of approximation is in order but, thanks to the formalism we are using, it can be a specialized one. As the path integration has been reduced to paths belonging to the same class, we can develop a different approximation, the most suitable, for each class!

In more detail, as only paths with average point $\bar{q}$ contribute to the path integral (2.21), in the action (2.18) we replace $V\big(q(u)\big)$ with a trial potential quadratic in the displacement from the average point

$$V_0(q;\bar{q}) = w(\bar{q}) + \tfrac{1}{2}m\omega^2(\bar{q})\,(q-\bar{q})^2 \tag{2.23}$$

where the parameters $w = w(\bar{q})$ and $\omega^2 = \omega^2(\bar{q})$ are now to be optimized so that the trial reduced density $\bar{\rho}_0(q;\bar{q})$ at best approximates $\bar{\rho}(q;\bar{q})$ *for each value of* $\bar{q}$.

The explicit evaluation of $\bar{\rho}_0(q;\bar{q})$ (see appendix B) gives

$$\bar{\rho}_0(q;\bar{q}) = \sqrt{\frac{m}{2\pi\hbar^2\beta}}\,\mathrm{e}^{-\beta w}\,\frac{f}{\sinh f}\left(\frac{1}{\sqrt{2\pi\alpha}}\,\mathrm{e}^{-(q-\bar{q})^2/2\alpha}\right) \tag{2.24}$$

with

$$\alpha = \alpha(\bar{q}) \equiv \frac{\hbar}{2m\omega}\left(\coth f - \frac{1}{f}\right) \qquad f = f(\bar{q}) \equiv \tfrac{1}{2}\beta\hbar\omega(\bar{q}). \tag{2.25}$$

In equation (2.24) one immediately recognizes that, within our approximation, $\mathcal{P}(q;\bar{q})$ is the Gaussian enclosed in brackets and

$$\rho_{\rm eff}(\bar{q}) = \sqrt{\frac{m}{2\pi\hbar^2\beta}}\,\mathrm{e}^{-\beta V_{\rm eff}(\bar{q})} \tag{2.26}$$

with the *effective potential*

$$V_{\rm eff}(\bar{q}) \equiv w(\bar{q}) + \frac{1}{\beta}\ln\frac{\sinh f(\bar{q})}{f(\bar{q})}. \tag{2.27}$$

Eventually, the average (2.22) becomes

$$\langle\mathcal{O}(\hat{q})\rangle = \frac{1}{\mathcal{Z}}\sqrt{\frac{m}{2\pi\hbar^2\beta}}\int \mathrm{d}\bar{q}\,\mathrm{e}^{-\beta V_{\rm eff}(\bar{q})}\left(\frac{1}{\sqrt{2\pi\alpha}}\int \mathrm{d}\xi\,\mathrm{e}^{-\xi^2/2\alpha}\;\mathcal{O}(\bar{q}+\xi)\right) \tag{2.28}$$

where $\xi \equiv q-\bar{q}$ replaces the variable q; as a consequence, no confusion arises if we *rub out the bar on* $\bar{q}$. We use a double angle bracket to denote the Gaussian average over the pure quantum fluctuations defined by $\mathcal{P}$, so that we rewrite the last equation as

$$\langle\mathcal{O}(\hat{q})\rangle = \frac{1}{\mathcal{Z}}\sqrt{\frac{m}{2\pi\hbar^2\beta}}\int \mathrm{d}q\;\langle\!\langle\mathcal{O}(q+\xi)\rangle\!\rangle\,\mathrm{e}^{-\beta V_{\rm eff}(q)}. \tag{2.29}$$

This equation constitutes the result of a rigorous derivation along the ideas developed at the end of the preceding subsection: in particular it is to be underlined that the variance α, heuristically introduced as $\alpha = \alpha_{\rm Q} - \alpha_{\rm C}$, turns out to be just that difference, but it is now well defined as a formal result. An essential condition for expression (2.29) to be meaningful is that $\alpha(q)$ remains positive for any q. As a function of temperature, α is positive and decreasing, taking the value $\hbar/(2m\omega)$ at $T=0$ and vanishing as $\hbar^2\beta/(12m)$ for $T \to \infty$.

Now, in order to close the approximation scheme, we still have to devise an optimization criterion for the parameters $w(q)$ and $\omega^2(q)$.

2.3. The pure quantum self-consistent harmonic approximation

After the choice (2.23) of the trial potential, one could try to make use of the same ideas underlying the usual HA and SCHA, taking into account that, as a new essential feature of the method, both w and ω^2 are functions of the position. For the HA, we simply identify the trial potential (2.23) with the expansion of $V(q)$ up to second order: this amounts to requiring that $w(q) = V(q)$ and $\omega^2(q) = V''(q)$ for any q. This recipe can be called the pure quantum HA. This is surely an improvement over the HA discussed in section 2.1, but in many cases it can lead to unphysical results [4]. Indeed it can happen that $V''(q)$ is negative: in this case $\alpha(\omega)$ can be analytically continued and in terms of the 'dimensionless frequency' $f = \beta\hbar\omega/2$ one has $\alpha = (\beta\hbar^2/4m)(\coth f/f - 1/f^2)$; if f^2 is negative, setting $f = i\varphi$, one has $\alpha = (\beta\hbar^2/4m)(1/\varphi^2 - \cot\varphi/\varphi)$, which diverges to $+\infty$ for $\varphi \to \pi^-$ (or $f^2 \to -\pi^2$) and is negative for $\varphi > \pi$ ($f^2 < -\pi^2$). As a consequence, if $\omega^2(q)$ is negative, at sufficiently low temperature we have $f^2 < -\pi^2$ and the pure quantum HA breaks down.

We then come back to the SCHA conditions (2.8) to push them down at the pure quantum level, eventually defining the pure quantum SCHA, or PQSCHA:

$$\begin{aligned} \langle\langle V(q+\xi)\rangle\rangle &= \langle\langle V_0(q+\xi)\rangle\rangle \equiv w(q) + \frac{m}{2}\omega^2(q)\,\alpha(q) \\ \langle\langle V''(q+\xi)\rangle\rangle &= \langle\langle V_0''(q+\xi)\rangle\rangle \equiv m\,\omega^2(q). \end{aligned} \tag{2.30}$$

Here the equation for the first derivative has been omitted, as possible linear terms of the trial potential do not contribute to the action. Once this self-consistent system has been solved, we have all the necessary ingredients to explicitly evaluate the effective potential and all the thermal averages through the classical-like expression (2.29). It is seen that for the most usual potentials the self-consistent solution for $\alpha(q)$ turns out to be always positive, even though $\omega^2(q)$ can be negative [4, 5].

We can now carry on a deeper discussion of the final results we expect to obtain by means of this method: from (2.22), where the separation between the classical and the pure quantum contributions has been performed, it should be already clear that the classical behaviour will be exactly described, whatever the approximations used in evaluating the residual path integral. In other terms, the specific choice of that approximation only affects the pure quantum contribution to the thermodynamics of the system; in particular, as we have used a quadratic approximation for the trial potential, we expect to describe exactly also the pure quantum harmonic contribution. In the definition of the effective potential (2.27) a logarithmic term appears, in the same form as the difference between the quantum and the classical free energy of a harmonic oscillator with frequency $\omega(q)$. That term assures that the harmonic free energy is exactly reproduced.

It is to be noticed that the PQSCHA and the SCHA are equivalent in the zero-temperature limit, where *quantum* and *pure quantum* become the same thing as any classical fluctuation is suppressed. It is less trivial, but perhaps even more interesting, to verify that applying the quantum SCHA one gets, at any temperature, the very same results that would have been obtained applying the classical SCHA to the pseudo-classical system described by V_{eff} [7].

Example. Let us now apply the PQSCHA to the quartic potential (2.14). Equations (2.30) and (2.27) give

$$\begin{aligned} \omega^2(q) &= \omega_0^2 + 12\lambda[q^2 + \alpha(q)] \\ V_{\text{eff}}(q) &= \frac{1}{2}\omega_0^2 q^2 + \lambda[q^4 - 3\alpha^2(q)] + \frac{1}{\beta}\ln\frac{\sinh f(q)}{f(q)} \end{aligned} \tag{2.31}$$

and the first one, self-consistently with the definition (2.25), determines the parameter $\omega^2(q)$ and hence the effective potential.

In figure 2 we again consider the normalized configuration density $P(q) = \langle \delta(q - \hat{q}) \rangle$, comparing the various approximations with the exact result, for two different temperatures. The explicit expression of the PQSCHA density [99] is found from equation (2.28) to be

$$P(q) = \frac{1}{\mathcal{Z}} \sqrt{\frac{m}{2\pi\hbar^2\beta}} e^{-\beta V_L(q)} \tag{2.32}$$

where the *local* effective potential $V_L(q)$ is defined by

$$e^{-\beta V_L(q)} = \int d\xi \, e^{-\beta V_{eff}(q+\xi)} \frac{1}{\sqrt{2\pi\alpha(q+\xi)}} e^{-\xi^2/2\alpha(q+\xi)}. \tag{2.33}$$

Note that, at variance with the HA and the SCHA, the PQSCHA density is not constrained to be a Gaussian and is indeed superior in all cases: at $T = 2$ it is practically indistinguishable from the exact result! While both the HA and the SCHA worsen on raising the temperature, the PQSCHA becomes better and better.

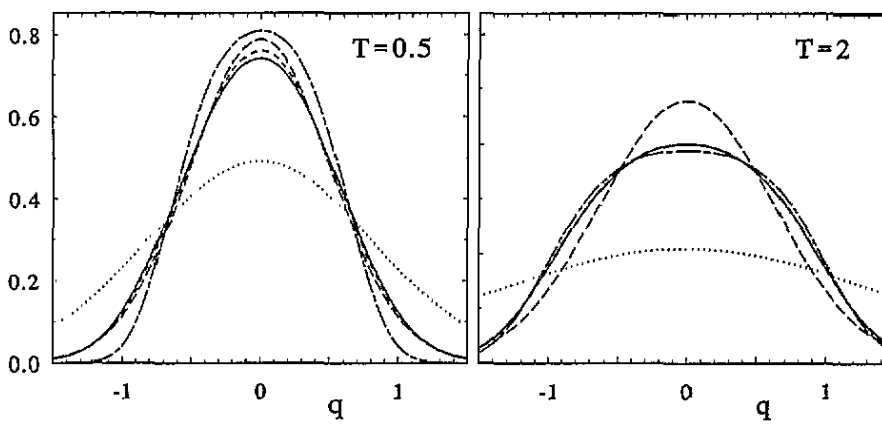

Figure 2. Normalized configuration probability distribution $P(q) = \langle \delta(q - \hat{q}) \rangle$ for the quartic oscillator (2.14) with $\omega_0 = 1$, $\lambda = 1$, at temperature $T = 0.5$ and $T = 2$. In the latter case the PQSCHA curve can hardly be distinguished from the exact one. Solid lines: exact quantum result; short dashed: PQSCHA; long dashed: quantum SCHA; dotted: quantum HA; dash–dotted: classical.

2.4. The variational method

We have already noticed that the very same results as from the SCHA, both in the classical and in the quantum case, can be obtained through a variational approach; this is still true in the pure quantum case, although some essential differences make the PQSCHA a more general method with respect to the previous variational one.

The variational approach is based on the so called Peierls–Jensen–Feynman inequality

$$F \leqslant F_0 + \frac{1}{\beta} \langle S_0 - S \rangle_{S_0} \tag{2.34}$$

where S is the true Euclidean action of the system under investigation, and S_0 a trial one, the functional average $\langle \cdots \rangle_{S_0}$ being taken among all closed paths with weight $\exp\{S_0[q(u)]\}$. Feynman's fundamental idea is the same as that we have borrowed and used to derive the

PQSCHA, namely that of classifying paths by the equivalence relation of having the same average point, in order to decompose the path integral.

At this point, instead of defining the reduced density, Feynman directly jumped to the introduction of a trial action S_0, letting it be a nonlocal functional through the dependence of its parameters on $\bar{q}$. The simplest choice of a free particle action

$$S_0[q(u)] = -\frac{1}{\hbar}\int_0^{\beta\hbar} \mathrm{d}u\ \frac{\dot{q}^2(u)}{2m} - \beta w(\bar{q}) \tag{2.35}$$

led him to a first effective potential that, though successfully applied to the polaron problem, lacks the desirable property of exactly describing the harmonic oscillator behaviour. Indeed it corresponds to set $\omega^2 \equiv 0$, imposing only the first of equations (2.30) so that α is found to be $\alpha = \hbar^2\beta/(12m)$ and the effective potential does not contain the logarithmic term.

The great improvement has been achieved [3, 4, 5] with the resort to a quadratic trial action

$$S_0[q(u)] = -\frac{1}{\hbar}\int_0^{\beta\hbar} \mathrm{d}u \left\{\frac{\dot{q}^2(u)}{2m} + \frac{1}{2}m\omega^2(\bar{q})\Big[q(u) - \bar{q}\Big]^2\right\} - \beta w(\bar{q}) \tag{2.36}$$

where $\bar{q}$ is meant as the average point functional (2.19), leading to results identical to the PQSCHA.

What is perhaps less transparent in the variational derivation is the actual meaning of the dependence of w and ω^2 on the average point $\bar{q}$: although it is clear that such a dependence makes S_0 a nonlocal functional and allows us then to look for the best approximation of the true action in a richer reservoir of mathematical objects, it is not immediately apparent that what one is actually doing is to develop a different approximation for each different class of paths. To make the variational approach suitable also in the nonstandard case, one has not only to introduce the Hamiltonian formalism of the path integral, but also to check that Feynman's inequality can be generalized to this formalism, thus providing the necessary variational principle. Unfortunately this is not the case, as Feynman's inequality is rigorously valid just in the standard case, although it is sensible to think that it could be at least verified for some class of nonstandard systems, and such a conjecture could be (and has been) used in some specific situations. As a matter of fact, however, there does not exist at the moment any variational principle safely available in the general nonstandard case, and this makes the PQSCHA approach a fundamental tool.

2.5. Application to some nonlinear potentials

In order to quantify the strength of the quantum character of a system described by the Hamiltonian (2.1) with a given potential $V(\hat{q})$, it is convenient to devise its characteristic energy scale ε (e.g., the barrier height for a double-well potential, the well depth for physical potentials that vanish at infinity, etc) and length scale σ (such that variations of V comparable to ε occur on this length scale) and write $V(\hat{q}) = \varepsilon v(\hat{q}/\sigma)$. In this way one better deals with a dimensionless coordinate $\hat{x} = \hat{q}/\sigma$. If x_m is the absolute minimum of $v(x)$, the system is characterized by the HA frequency $\omega_0 = \sqrt{\varepsilon\gamma^2/m\sigma^2}$, with $\gamma^2 = v''(x_m)$, and a dimensionless coupling parameter g for the system can be defined as the ratio between the HA quantum energy level splitting $\hbar\omega_0$ and the overall energy scale ε,

$$g = \frac{\hbar\omega_0}{\varepsilon} = \sqrt{\frac{\hbar^2 v''(x_m)}{m\varepsilon\sigma^2}}. \tag{2.37}$$

The case of weak (strong) quantum effects occurs when g is small (large) compared to unity. In the following applications we shall make use of the dimensionless variables only,

i.e. energies are given in units of ε, lengths in units of σ, frequencies in units of ω_0 and so on; the reduced temperature is $t = 1/(\varepsilon\beta)$.

2.5.1. The double-well quartic potential. This potential is

$$v(x) = (1 - x^2)^2 \tag{2.38}$$

with two symmetric minima in $x_m = \pm 1$. From the PQSCHA equations (2.30) and the definitions (2.27) and (2.25) we obtain

$$v_{\text{eff}}(x) = (1 - x^2)^2 - 3\alpha^2(x) + t \ln \frac{\sinh f(x)}{f(x)}$$

$$f^2(x) = \frac{g^2}{8t^2}(3x^2 - 3\alpha(x) - 1)$$

$$\alpha(x) = \frac{g^2}{32t}\frac{1}{f(x)}\left(\coth f(x) - \frac{1}{f(x)}\right).$$

The last two equations have to be solved self-consistently. This task is done numerically, and exact reference data can be obtained by numerical solution of the stationary Schrödinger equation.

In figure 3 we report a comparison concerning the local effective potential (2.33), $V_L(q) \equiv \varepsilon v_L(q/\sigma)$, that describes in a direct classical-like way the configuration density; in terms of the effective potential it is given by the integral

$$e^{-\beta V_L(q)} = \int d\xi \frac{1}{\sqrt{2\pi\alpha(q+\xi)}} e^{-\xi^2/2\alpha(q+\xi)} e^{-\beta V_{\text{eff}}(q+\xi)}. \tag{2.39}$$

High values of the coupling have been chosen in figure 3, in order to show how in the strongly quantum regime the PQSCHA can still reproduce extremely well the exact data.

We refer to the literature for further details on the PQSCHA of the quartic double well [4, 5, 99, 29]. Interesting singular potentials for which the effectiveness of the PQSCHA has been tested [30] are the Dirac delta potential $v(x) = -\delta(x)$, the harmonic plus delta potential $v(x) = x^2/2 - \delta(x)$ [100], the one-dimensional Coulomb potential $|x|/2$, the Morse potential $v(x) = (e^{-x} - 1)^2$. In [30] one can also find a discussion about the high-temperature expansion of the effective potential.

An interesting application of these one-particle results has been made for calculating the order parameter of ferroelectrics [101]. At variance with the SCHA calculation, the effective potential method can describe the behaviour of the order parameter up to the transition temperature.

2.5.2. Central potential in three dimensions. In the case of a central potential $V(q)$ in three dimensions ($q \equiv |\boldsymbol{q}|$) it is possible to reduce the computations to the case of one degree of freedom. Indeed the angular part of the quantum problem can be separated and solved exactly. Exploiting this fact the particle density can be written as

$$\rho(q) = \frac{1}{4\pi q^2}\sum_{\ell=0}^{\infty}(2\ell + 1)\rho_\ell(q) \tag{2.40}$$

where $\rho_\ell(q) \equiv \langle q|e^{-\beta\hat{\mathcal{H}}_\ell}|q\rangle$ are the one-dimensional particle densities for the Hamiltonians

$$\hat{\mathcal{H}}_\ell = \frac{p^2}{2m} + V_\ell(q) = \frac{p^2}{2m} + V(q) + \frac{\hbar^2\ell(\ell+1)}{2mq^2} \tag{2.41}$$

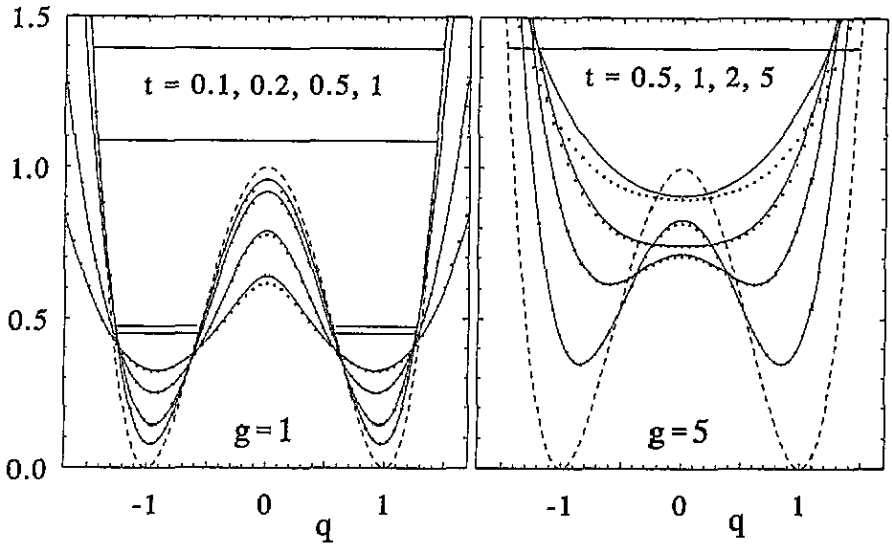

Figure 3. The *local* effective potential $v_L(x)$ (see text) of the quartic double well, at different temperatures, for quantum coupling $g = 1$ and $g = 5$. Solid lines are the PQSCHA result and dots are the exact data. On raising t the local effective potential tends towards the original one (dashed line). The exact energy levels are also reported by horizontal lines.

that describe the separated contributions of different values of the angular momentum. In principle, an infinite number of $\rho_\ell(q)$ has to be calculated. However the centrifugal term makes their values less and less relevant for increasing ℓ, in such a way that the series (2.40) converges exponentially rapidly.

The same approach can be used for the central interaction of two particles, after the separation of the centre-of-mass motion, in terms of the relative coordinate and the reduced mass. A coupling constant is naturally introduced as in equation (2.37). In figure 4 we report the results obtained in the case of a Lennard-Jones potential model $v(x) = 4(x^{-12} - x^{-6})$, with the parameters $\varepsilon = 36.7$ K and $\sigma = 2.959$ Å suitable for describing the interaction of hydrogen molecules ($m = 2.01$ uma). The resulting coupling $g = 2.93$ tells us that this is a strongly quantum system, as witnessed by the comparison with the classical limit and by the inadequacy of the quantum corrections introduced by the Wigner expansion [13, 17, 14, 102, 103]. For a deeper discussion of this system and details about the regularization of the diverging integrals arising from the singularity of the potential, see [36].

A similar system, the Coulomb potential in three dimensions, is analysed by PQSCHA in [28].

3. Standard systems—many degrees of freedom

The previous section has shown that the PQSCHA is quite effective in treating simple one-particle quantum systems. Of course, in order to make the method useful for interesting problems and realistic physical models, the successive step is the extension of the formalism to the many-particle case. Therefore, let us consider a general system with M degrees of freedom, i.e. canonical coordinate and momentum operators $\hat{q} \equiv \{\hat{q}_\mu\}_{\mu=1,\dots,M}$ and $\hat{p} \equiv \{\hat{p}_\mu\}_{\mu=1,\dots,M}$, with the commutation relations $[\hat{q}_\mu, \hat{p}_\nu] = i\delta_{\mu\nu}$ (we set $\hbar = 1$ from

now on), and described by the standard Hamiltonian

$$\hat{\mathcal{H}} = \tfrac{1}{2}\hat{\boldsymbol{p}}^{\mathrm{T}}\boldsymbol{A}^2\hat{\boldsymbol{p}} + V(\hat{\boldsymbol{q}}) = \frac{1}{2}\sum_{\mu,\nu=1}^{M}\hat{p}_\mu A^2{}_{\mu\nu}\hat{p}_\nu + V(\hat{\boldsymbol{q}}). \tag{3.1}$$

As the matrix $\boldsymbol{A}^2 = \{A^2{}_{\mu\nu}\}$ is real symmetric and positive definite, there exist its positive square root $\boldsymbol{A}$ and its inverse $\boldsymbol{A}^{-1}$.

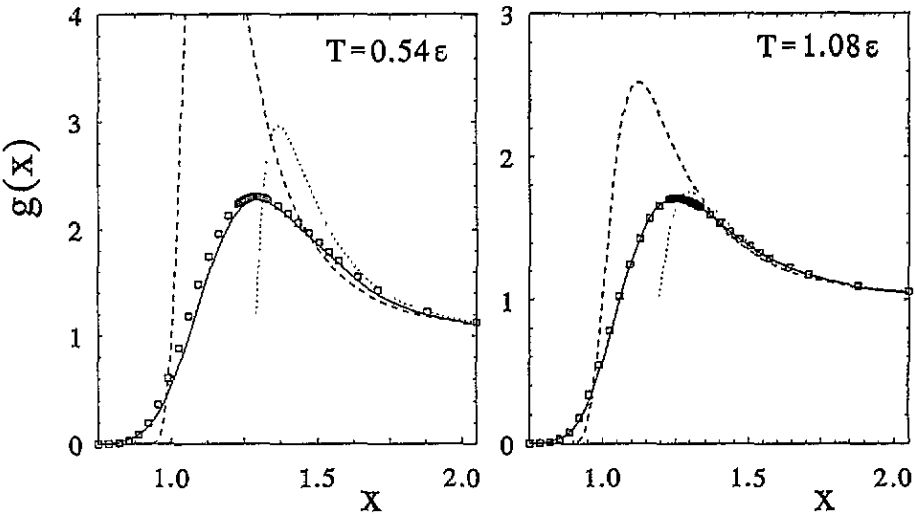

Figure 4. The pair correlation function $g(r)$ for the Lennard-Jones interaction model for two hydrogen molecules at the temperatures $T = 0.54\varepsilon \simeq 20$ K and $T = 1.08\varepsilon \simeq 40$ K. Solid lines are the PQSCHA result and the squares are numerically obtained exact data [104]. The dashed lines report the classical result, and the dotted ones are the high-temperature approximation from the Wigner expansion.

The corresponding path integral for the equilibrium configuration density at temperature β^{-1} is now a sum over paths $\boldsymbol{q}(u)$ in the M-dimensional configuration space,

$$\rho(\boldsymbol{q}) \equiv \langle \boldsymbol{q}|\, \mathrm{e}^{-\beta\hat{\mathcal{H}}}\, |\boldsymbol{q}\rangle = \int_{\boldsymbol{q}}^{\boldsymbol{q}} \mathcal{D}[\boldsymbol{q}(u)]\ \mathrm{e}^{S[\boldsymbol{q}(u)]} \tag{3.2}$$

where the action is

$$S[\boldsymbol{q}(u)] = -\int_0^\beta \mathrm{d}u\left[\tfrac{1}{2}\dot{\boldsymbol{q}}^{\mathrm{T}}(u)\boldsymbol{A}^{-2}\dot{\boldsymbol{q}}(u) + V\big(\boldsymbol{q}(u)\big)\right] \tag{3.3}$$

and the measure of the path integral includes a factor $\left[(2\pi\beta/P)^{M/2}\det \boldsymbol{A}\right]^{-P}$ in the discretized version with P imaginary time slices.

3.1. The PQSCHA

Let us now generalize the single-particle framework of the PQSCHA. The average point functional in the M-dimensional configuration space is $(1/\beta)\int_0^\beta \mathrm{d}u\ \boldsymbol{q}(u)$. The reduced density

$$\tilde{\rho}(\boldsymbol{q};\bar{\boldsymbol{q}}) = \int_{\boldsymbol{q}}^{\boldsymbol{q}} \mathcal{D}[\boldsymbol{q}(u)]\ \delta\left(\bar{\boldsymbol{q}} - \frac{1}{\beta}\int_0^\beta \mathrm{d}u\ \boldsymbol{q}(u)\right)\ \mathrm{e}^{S[\boldsymbol{q}(u)]} \tag{3.4}$$

is such that the density matrix is obtained by ordinary integration over $\bar{q}$,

$$\rho(q) = \int \mathrm{d}\bar{q}\ \bar{\rho}(q;\bar{q}). \tag{3.5}$$

The same argument as in section 2.3 leads us to approximate $V(q)$ by a quadratic polynomial in the deviation from $\bar{q}$,

$$V_0(q;\bar{q}) = w(\bar{q}) + \tfrac{1}{2}(q-\bar{q})^{\mathrm{T}}\boldsymbol{B}^2(q-\bar{q}). \tag{3.6}$$

Therefore, we have as parameters the scalar $w(\bar{q})$ and the $M(M+1)/2$ independent components of the symmetric matrix $\boldsymbol{B}^2(\bar{q}) = \{B^2{}_{\mu\nu}(\bar{q})\}$, replacing the previous scalar $m\omega^2(\bar{q})$. The trial reduced density $\bar{\rho}_0$ can be evaluated analytically as shown in appendix C. The calculation involves the diagonalization of the dynamical matrix $\boldsymbol{AB}^2\boldsymbol{A}$ by an orthogonal matrix $\boldsymbol{U}(\bar{q}) \equiv \{U_{k\mu}(\bar{q})\}$,

$$\sum\nolimits_{\mu\nu} U_{k\mu}(\boldsymbol{AB}^2\boldsymbol{A})_{\mu\nu}U_{\ell\nu} = \delta_{k\ell}\omega_k^2(\bar{q}). \tag{3.7}$$

The reduced configuration density $\bar{\rho}_0(q;\bar{q})$ turns out to be a Gaussian centred at $\bar{q}$. We then proceed as in section 2.2, introducing $\xi \equiv q-\bar{q}$ and *suppressing the bar* of $\bar{q}$. Equation (3.7) tells us that V_0 is diagonal in terms of the 'normal mode' variables $\xi_k = \sum_\mu \{\boldsymbol{UA}^{-1}\}_{k\mu}\xi_\mu$, where we distinguish between the original variables and their normal modes by the use of greek and latin indices, respectively, in order to maintain a self-contained notation. The Gaussian average $\langle\!\langle \cdots \rangle\!\rangle$ over ξ is defined by the moments

$$\langle\!\langle \xi_k\xi_\ell \rangle\!\rangle = \delta_{k\ell}\alpha_k(q) \tag{3.8}$$

where

$$\alpha_k(q) = \frac{1}{2\omega_k(q)}\left(\coth f_k(q) - \frac{1}{f_k(q)}\right) \qquad f_k(q) = \frac{1}{2}\beta\omega_k(q). \tag{3.9}$$

Now, the pure quantum fluctuations described by ξ appear to be properly taken for each normal mode.

As we know from the one-particle case, the PQSCHA consists in imposing SCHA conditions on the reduced density $\bar{\rho}_0$,

$$\langle\!\langle V(q+\xi) \rangle\!\rangle = \langle\!\langle V_0(q+\xi) \rangle\!\rangle = w(q) + \tfrac{1}{2}\sum\nolimits_k \omega_k^2(q)\,\alpha_k(q) \tag{3.10}$$

$$\langle\!\langle \partial_{q_\mu}\partial_{q_\nu} V(q+\xi) \rangle\!\rangle = \langle\!\langle \partial_{q_\mu}\partial_{q_\nu} V_0(q+\xi) \rangle\!\rangle = B^2{}_{\mu\nu}(q). \tag{3.11}$$

The first equation determines $w(q)$ and the second one, that has a self-consistent solution together with (3.7), determines at the same time the matrix $\boldsymbol{B}^2(q)$ and the moments (3.8). The average of a configuration dependent observable $\mathcal{O}(\hat{q})$ is approximated (see appendix C) by the classical-like formula

$$\langle \mathcal{O}(\hat{q}) \rangle = \frac{1}{\mathcal{Z}}\frac{1}{(2\pi\beta)^{M/2}\det \boldsymbol{A}}\int \mathrm{d}q\ \langle\!\langle \mathcal{O}(q+\xi) \rangle\!\rangle\ \mathrm{e}^{-\beta V_{\mathrm{eff}}(q)} \tag{3.12}$$

with the effective potential

$$V_{\mathrm{eff}}(q) = \langle\!\langle V(q+\xi) \rangle\!\rangle - \frac{1}{2}\sum\nolimits_k \omega_k^2(q)\,\alpha_k(q) + \frac{1}{\beta}\sum\nolimits_k \ln\frac{\sinh f_k(q)}{f_k(q)}. \tag{3.13}$$

The above framework is also obtained [3, 5] by minimizing the right-hand side of Feynman's inequality (2.34) [2, 68]. The physical interpretation of equation (3.12) parallels the one we have already made in section 2.3. The pure quantum fluctuations are approximated as a multidimensional Gaussian with variance $\alpha_k(q)$ for each normal mode; we will call its (correlated) moments in direct space *renormalization parameters*

$$D_{\mu\nu}(q) = \langle\!\langle \xi_\mu\xi_\nu \rangle\!\rangle = \sum\nolimits_k \{\boldsymbol{UA}\}_{k\mu}\{\boldsymbol{UA}\}_{k\nu}\,\alpha_k. \tag{3.14}$$

It is easy to express the double-bracket averages like those appearing in equations (3.10), (3.11), (3.12), and (3.13), in terms of a (usually limited) number of the $D_{\mu\nu}(q)$, using the well known properties of Gaussian distributions.

Let us introduce a shorthand notation by means of the q-dependent second-order differentiation operator

$$\Delta(q) \equiv \tfrac{1}{2}\langle\!\langle(\xi^{\mathrm{T}}\partial_q)^2\rangle\!\rangle = \tfrac{1}{2}\sum_{\mu\nu} D_{\mu\nu}(q)\,\partial_{q_\mu}\partial_{q_\nu}. \tag{3.15}$$

It is easily seen that, if the $D_{\mu\nu}(q)$ are understood to be unaffected by Δ,

$$\langle\!\langle \mathcal{O}(q+\xi)\rangle\!\rangle = \mathrm{e}^{\Delta(q)}\,\mathcal{O}(q). \tag{3.16}$$

This exponential gives rise to a power series (in the D) that parallels the Hartree–Fock resummation of one-loop diagrams, and turns out to be very useful in practical calculations. With this notation (see appendix C) the effective potential can be written as

$$V_{\mathrm{eff}}(q) = \bigl[1-\Delta(q)\bigr]\mathrm{e}^{\Delta(q)}\,V(q) + \frac{1}{\beta}\sum\nolimits_k \ln\frac{\sinh f_k(q)}{f_k(q)} \tag{3.17}$$

where it appears that the correction to $V(q)$ from the first term is of second order in the D, since $(1-\Delta)\mathrm{e}^{\Delta} \sim \Delta^2$.

3.2. The low-coupling approximation

As in the case of one degree of freedom only, the implementation of the method requires a self-consistent solution of a set of equations, for any value of q. This task becomes very difficult for a many-particle system, since solving the set of equations (3.7), (3.8), (3.9) and (3.11) could become numerically as heavy as affording the same system by quantum Monte Carlo simulation. Therefore, a further simplification is in order. So, let us analyse the form of the fundamental formula, equation (3.12). It is apparent that, at low temperatures, the main contribution to the configuration integral arises from the neighbourhood of the minimum q_0 of $V_{\mathrm{eff}}(q)$. In this regime we could then safely approximate the renormalization parameters $D_{\mu\nu}(q)$ (or $\alpha_k(q)$, i.e. the pure quantum fluctuations) starting from their values in q_0. On the other hand, when the temperature rises, the renormalization parameters decrease, becoming less and less relevant; in particular, for $f_k \gg 1$, $\alpha_k(q) \sim \beta\hbar^2/12$ and loses its configuration dependence, so that such an approximation would have little effect.

Therefore, we are led to introduce what has been called the *low-coupling approximation* (LCA). We expand the dynamical matrix $B^2(q)$ around the minimum q_0 of $V_{\mathrm{eff}}(q)$,

$$B^2(q) = B^2 + \delta B^2(q) \tag{3.18}$$

where $B^2 \equiv B^2(q_0)$, and consequently we expand the frequencies $\omega_k^2(q) = \omega_k^2 + \delta\omega_k^2(q)$, the orthogonal matrix $U(q) = U + \delta U(q)$, and so on (for all quantities taken in q_0 we *omit the argument*). This allows us to deal with Gaussian averages $\langle\!\langle\cdots\rangle\!\rangle_0$ which do not depend any longer on the configuration: the self-consistent equations have to be solved only once, with a great simplification in implementing the method. After this expansion (see appendix D for details) the effective potential reduces to the simpler form

$$V_{\mathrm{eff}}(q) = \mathrm{e}^{\Delta}\,V(q) - \Delta\mathrm{e}^{\Delta}\,V(q_0) + \frac{1}{\beta}\sum\nolimits_k \ln\frac{\sinh f_k}{f_k} \tag{3.19}$$

and q_0 is the solution of $\mathrm{e}^{\Delta}\partial_q V(q) = 0$, since the other terms of V_{eff} are independent of q. Here, a self-consistency arises from the dependence on q_0 of the renormalization operator e^{Δ}. Actually, in most cases the solutions of this equation can be picked out by symmetry considerations.

The calculations are particularly easy in the case of a *translation invariant* system, with a translation invariant minimum: the matrix U is just a standard real Fourier transformation, which also diagonalizes the 'reciprocal mass' matrix A^2,

$$\sum_{\mu\nu} U_{k\mu} A^2{}_{\mu\nu} U_{\ell\nu} = m_k^{-1}\, \delta_{k\ell} \tag{3.20}$$

and the renormalization parameters can be written as

$$D_{\mu\nu} = \sum_k U_{k\mu} U_{k\nu}\, m_k^{-1}\, \alpha_k. \tag{3.21}$$

Using this expression, the LCA effective potential (3.19) can be easily obtained from the true one, $V(q)$. Only a reduced set of the renormalization parameters will be explicitly needed in V_{eff}. For instance, an additive local interaction term in $V(q)$ like $V_1(q) = \sum_\mu v(q_\mu)$ involves the only renormalization parameter $D_0 = D_{\mu\mu}$ (due to translation symmetry, it is independent of μ),

$$D_0 = \sum_k \frac{1}{2m_k\omega_k}\left(\coth f_k - \frac{1}{f_k}\right). \tag{3.22}$$

Indeed, $\Delta v(q_\mu) = D_{\mu\mu}\partial^2_{q_\mu} v(q_\mu)$, so that it is immediate to get

$$\mathrm{e}^{\Delta}\, V_1(q) - \Delta \mathrm{e}^{\Delta}\, V_1(q_0) = \sum_\mu \sum_{n=0}^{\infty} \frac{1}{n!}\left[v^{(2n)}(q_\mu) - n\, v^{(2n)}(q_{0,\mu})\right]\left(\frac{D_0}{2}\right)^n \tag{3.23}$$

where $v^{(2n)}$ is the $2n$th derivative of $g(q_\mu)$. This example can be easily generalized to other kinds of interaction term, with the possible appearance of a few different D, which are the only ones to be determined (for instance, by an iterative method), because only they appear in the right-hand side of the LCA version of equation (3.11). Moreover, their evaluation has to be performed only once at a given temperature. Therefore, by the LCA we benefit from the great advantage that the effective potential can be directly used in classical-like calculations. This means that any known classical results and methods can be applied, and, e.g., classical Monte Carlo computations can be used. In addition, improvements of the LCA are possible, for instance by accounting at lowest order for the corrections to the renormalization parameters [78].

It is apparent that for a harmonic potential the exact results are still recovered in the LCA. As for the comparison with the SCHA, one can verify that there is still full agreement at zero temperature. Note that the effect of the classical part of the fluctuations on the renormalizations themselves has been disregarded. Moreover, it has been shown [30, 7] that in the high-T limit the above framework agrees, at least within order $\hbar^2\beta$, with the Wigner–Kirkwood expansion method [13, 15, 16, 17, 14].

3.3. More general averages and Weyl ordering

Let us face the problem of calculating averages of a general observable $\hat{\mathcal{O}}(\hat{p}, \hat{q})$, that depends on both canonical variables. The hat over $\hat{\mathcal{O}}$ tells us that we cannot regard it as a simple functional dependence on $(\hat{p}, \hat{q})$, since these variables do not commute. In order to write a classical-like expression for $\langle\hat{\mathcal{O}}\rangle$, we need a one-to-one rule for associating functions, defined in the phase space of points (p, q), to operators, acting in the Hilbert space of states of the system. There is arbitrariness in this choice, due to the infinite possible choices of ordering rules for the pairs $(\hat{p}_\mu, \hat{q}_\mu)$. Here we use *Weyl ordering* [14, 105], which associates to any operator $\hat{\mathcal{O}}$ a function $\mathcal{O}(p, q)$, called the *Weyl symbol* for $\hat{\mathcal{O}}$, in the following way:

$$\mathcal{O}(p, q) \equiv \int \mathrm{d}\zeta\, \mathrm{e}^{-\mathrm{i}p^{\mathrm{T}}\zeta} \langle q + \tfrac{1}{2}\zeta |\, \hat{\mathcal{O}}\, | q - \tfrac{1}{2}\zeta\rangle. \tag{3.24}$$

This rule satisfies a number of nice properties [14]. Among them, we recall that the trace of the product of two operators $\hat{\mathcal{O}}_1$ and $\hat{\mathcal{O}}_2$ coincides with the phase-space integral of the product $\mathcal{O}_1\mathcal{O}_2$

$$\mathrm{Tr}(\hat{\mathcal{O}}_1\,\hat{\mathcal{O}}_2) = \int \frac{\mathrm{d}p\,\mathrm{d}q}{(2\pi)^M}\,\mathcal{O}_1(p,q)\,\mathcal{O}_2(p,q) \tag{3.25}$$

and that $\mathcal{O}(p,q)$ is real if and only if $\hat{\mathcal{O}}$ is self-adjoint. The function $\mathcal{O}(p,q)$ is connected with the matrix elements of $\hat{\mathcal{O}}$ in the coordinate representation by

$$\mathcal{O}(q'',q') \equiv \langle q''|\,\hat{\mathcal{O}}\,|q'\rangle = \int \frac{\mathrm{d}p}{(2\pi)^M}\,\mathrm{e}^{\mathrm{i}p^{\mathrm{T}}(q''-q')}\,\mathcal{O}\Big(p,\frac{q'+q''}{2}\Big). \tag{3.26}$$

Note that the arguments are used to distinguish between the matrix elements $\mathcal{O}(q'',q')$ and the Weyl symbol $\mathcal{O}(p,q)$ for the operator $\hat{\mathcal{O}}$. It is sometimes useful to obtain the Weyl symbol from the *p-q symbol* $\mathcal{O}_{p\text{-}q}(p,q)$ [105] whose functional dependence is obtained by shifting all momentum operators to the left of the coordinate operators, taking into account their commutation rules,

$$\mathcal{O}(p,q) = \exp\Big(-\frac{\mathrm{i}}{2}\sum\nolimits_\mu \partial_{p_\mu}\partial_{q_\mu}\Big)\,\mathcal{O}_{p\text{-}q}(p,q). \tag{3.27}$$

The quantum thermal average of an observable $\hat{\mathcal{O}}$ being defined as $\mathrm{Tr}(\hat{\mathcal{O}}\hat{\rho})$, we have

$$\langle\hat{\mathcal{O}}\rangle = \frac{1}{\mathcal{Z}}\int \frac{\mathrm{d}p\,\mathrm{d}q}{(2\pi)^M}\,\mathcal{O}(p,q)\,\rho(p,q) \tag{3.28}$$

so we can find the wanted expression by calculating the Weyl symbol for the PQSCHA density matrix, as done at the end of appendix C, equation (C.10). Eventually, one gets the following PQSCHA expression for thermal averages:

$$\langle\hat{\mathcal{O}}(\hat{p},\hat{q})\rangle = \frac{1}{\mathcal{Z}}\left(\frac{2\pi}{\beta}\right)^{M/2}\frac{1}{\det A}\int \mathrm{d}q\;\mathrm{e}^{-\beta V_{\mathrm{eff}}(q)}\int \mathrm{d}p\,\langle\!\langle\mathcal{O}(p,q+\xi)\rangle\!\rangle\prod_k \frac{1}{\sqrt{2\pi\lambda_k}}\mathrm{e}^{-p_k^2/2\lambda_k} \tag{3.29}$$

where

$$\lambda_k = \lambda_k(q) = \tfrac{1}{2}\,\omega_k(q)\,\coth f_k(q). \tag{3.30}$$

By the average over the coordinates it appears that the momentum distribution $P(p) = \langle\delta(p-\hat{p})\rangle$ is not a Gaussian. However, in the LCA, where expression (3.29) is formally identical, it becomes Gaussian, since $\lambda_k \equiv \lambda_k(q_0)$ is fixed at its value in q_0.

4. Standard systems—applications

4.1. Kink bearing fields in one dimension

This has been the first application of the PQSCHA in a system with many degrees of freedom [3, 4, 41, 42, 43, 44, 45, 106, 107]. A Lorentz invariant Hamiltonian for a scalar one-dimensional field $\hat{\psi}(z)$ ($\hbar = c = 1$) is

$$\hat{\mathcal{H}} = \int \mathrm{d}z\left[\frac{\hat{\pi}^2}{2} + \frac{1}{2}\Big(\frac{\partial\hat{\psi}}{\partial z}\Big)^2 + \frac{\mu^2}{g^2}v(g\hat{\psi})\right] \tag{4.1}$$

where $v(q)$ is a local potential with $v''(q_{\mathrm{m}}) = 1$ in its absolute minimum q_{m}, μ is the 'field mass' and g^2 is the usual field theoretical coupling constant. $\hat{\pi}(z)$ is the momentum density, $\big[\hat{\psi}(z),\hat{\pi}(z')\big] = \mathrm{i}\delta(z-z')$. The low-energy excitations are quasi-particles with relativistic

energies $\varepsilon_k = \sqrt{\mu^2 + k^2}$. If the absolute minimum of $v(q)$ is degenerate, the classical field admits kink excitations that connect different minima. In particular we have the φ^4 model for $v(x) = (x^2 - 1)^2/8$ and the sine–Gordon (SG) model for $v(x) = (1 - \cos x)$, with classical kink energy $\varepsilon_K = 2\mu/3g^2$ and $\varepsilon_K = 8\mu/g^2$, respectively. The discretized version of the above model for a chain with spacing a and N sites is $\hat{\mathcal{H}} = (g^2/2a)\sum_i \hat{p}_i^2 + V(\hat{q})$, with

$$V(q) = \frac{a}{g^2}\sum_{i=1}^{N}\left[\frac{(q_i - q_{i-1})^2}{2a^2} + \mu^2 v(q_i)\right]. \tag{4.2}$$

The coordinates are $\hat{q} = \{\hat{q}_i = g\hat{\psi}(z_i)\}$ and their conjugate momenta $\hat{p} = \{\hat{p}_i = ag^{-1}\hat{\pi}(z_i)\}$. Equation (3.19) gives the LCA effective potential; it can be calculated using (3.23) in terms of the renormalization parameter $D_0(T)$, equation (3.22), with $m_k = ag^{-2}$ and $\omega_k^2 = \mu^2\kappa^2(T) + 4a^{-2}\sin^2(ka/2)$, where $\kappa^2(T)$ depends on $D_0(T)$. Eventually, $V_{\text{eff}}(q)$ is expressed as the original potential (4.2), with $v(q_i)$ replaced by a proper $v_{\text{eff}}(q_i)$. For the two models considered we have:

$$\kappa^2(T) = 1 - 3D_0 \qquad v_{\text{eff}}(x) = \tfrac{1}{8}(x^2 - 1 + 3D_0)^2 + \tfrac{3}{4}D_0^2 + H(T)(\varphi^4)$$
$$\kappa^2(T) = \mathrm{e}^{-D_0/2} \qquad v_{\text{eff}}(x) = \mathrm{e}^{-D_0/2}(1 - \cos x) + \tfrac{1}{8}D_0^2 + H(T)(\text{SG})$$

where $H(T) = [\mu^2 a^2/(g^2 N\beta)]\sum_k \ln(\sinh f_k/f_k)$. The quantum thermodynamic quantities can be then obtained by numerical transfer matrix [108], making their calculation not only feasible, but also very easy. The results are reliable as long as the Ginzburg condition $v_{\text{eff}}^{(4)}(q_0)D_0(T)/2\kappa(T) \ll 1$ is satisfied; if the coupling is strong enough, it breaks at sufficiently low T. The reasonability of this criterion has been recently proven through a check against accurate quantum Monte Carlo data for the φ^4 chain [109]. The cited paper also proves the enormous amount of simplification obtained by the PQSCHA, since the quite long Monte Carlo runs made in order to get accuracy for the internal energy turned out to display a considerable statistical error on the specific heat.

Furthermore, we would like to note that the PQSCHA approach to the SG chain model justifies and improves an earlier [110] rearrangement of the high-T expansion, made by adding the (bare) harmonic behaviour and simultaneously subtracting the corresponding terms from the series.

The PQSCHA approach also permits analytical work, and in the case of the sine–Gordon and of the φ^4 fields all the results that were obtained by specializing the quantum SCHA to the vacuum and the one-kink sectors [111, 112, 113] are naturally recovered by performing the classical SCHA with the effective model [43, 44], starting from the absolute minimum and from the one-kink configuration.

In the continuum limit $D_0(T) \to \infty$ and one replaces the bare field mass μ with its zero-T renormalized counterpart $\mu_0 = \mu\kappa(0)$, obtaining a formally identical expression of $v_{\text{eff}}(q)$ up to order g^4, in terms of the finite renormalization parameter $D'(T) = D(T) - D(0)$. In the φ^4 case the coupling constant has to be renormalized as well [45]. In figure 5 we report a comparison with quantum Monte Carlo data and exact Bethe *ansatz* results for a quantity that is very sensitive to nonlinearity, namely the excess specific heat (that is the difference between the specific heat and its counterpart in the harmonic approximation). The PQSCHA turns out to be complementary to the Bethe *ansatz*, whose equations are affordable only for very high values of the coupling [114].

We refer to the papers quoted at the beginning of this subsection for a deeper discussion.

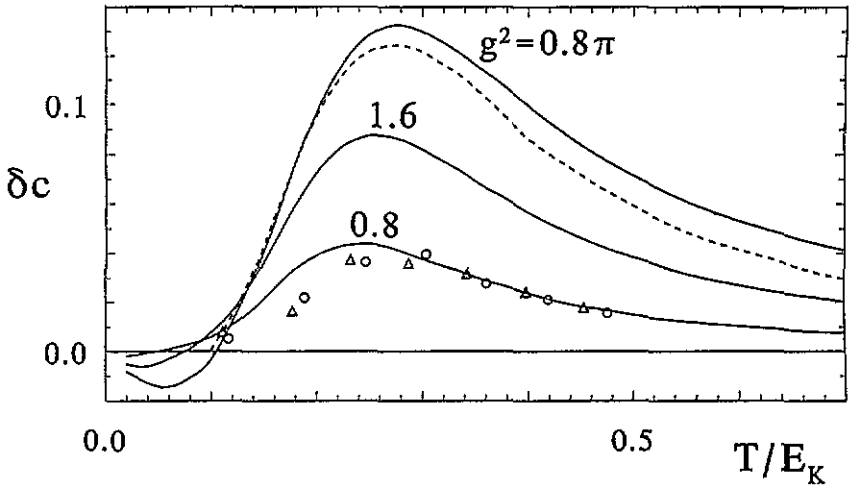

Figure 5. Nonlinear contribution to the specific heat density against temperature for the sine-Gordon field. The length unit has been chosen according to the convention $\hbar = c = E_K = 1$. Solid lines: PQSCHA data for different values of g^2. Dashed line: Bethe *ansatz* exact results from [114] for the lowest available coupling $g^2 = 0.8\pi$. For this strong coupling the difference agrees with the estimation of the terms $\sim g^4$ that are neglected in the LCA [45]. Symbols: quantum Monte Carlo data for $g^2 = 0.8$, at 'discreteness' parameter $\mu a = 0.34$ (triangles) and 0.10 (circles) from [66], properly scaled as discussed in [45].

4.2. Toda and Lennard-Jones chains

One-dimensional (1D) systems of atoms tightened together by nonlinear forces represent the field of application where the effective potential method displays at best all of its power. In fact, apart from the almost trivial case of a single particle, in 1D systems we get the biggest gain by the use of the effective potential. The actual computational effort needed to evaluate quantum thermodynamic properties, which by Trotter decomposition is easily shown to be equivalent to that of a 2D classical system, is in fact brought back to that of a classical 1D problem. And for the latter different methods, both numerical [108] and analytical [115, 77] are available to evaluate, in principle exactly, the partition function and other relevant static quantities. In this section, we give a survey of the applications of the effective potential method to systems where the interaction is only between nearest neighbours, i.e.

$$V(q) = \sum_\mu v(q_\mu - q_{\mu-1}). \tag{4.3}$$

For such systems, within the LCA, the effective potential may be written again as a sum of pairwise interactions, $V_{\rm eff}(q) = \sum_\mu v_{\rm eff}(q_\mu - q_{\mu-1})$, where

$$v_{\rm eff}(r) = \sum_\ell \frac{1}{\ell!}\left[v^{(2\ell)}(r) - \ell v^{(2\ell)}(d)\right]\left(\frac{D_1}{2}\right)^\ell + H(T) \tag{4.4}$$

$$D_1 \equiv 2(D_{\mu\mu} - D_{\mu\mu+1}) = \frac{1}{m}\sum_k 4\sin^2(kd/2)\,\alpha_k \tag{4.5}$$

being the renormalization parameter typical of one-dimensional systems with nearest-neighbour interaction only, and d the lattice constant, i.e. the thermal equilibrium average distance between two neighbouring particles.

As a first example of a nonlinear chain we consider the Toda lattice. Such a model lattice is known to be exactly integrable both in the classical [116, 117, 118] and quantum case [119], and even if dynamical integrability does not imply necessarily that also thermodynamic quantities can be exactly evaluated, the exact partition function of the Toda lattice is known in analytic form for the classical system [120], and has been obtained numerically for the quantum one by the Bethe *ansatz* [121, 122, 123, 124, 125], so that reference data are available to appreciate the value of the effective potential method.

The nearest-neighbour interaction potential introduced by Toda is

$$v(r) = \frac{a}{b}\left[e^{-b(r-r_0)} - 1\right] + a(r - r_0). \tag{4.6}$$

r_0 is the position of the minimum of $v(r)$, the constant b rules the nonlinearity of the potential, while the ratio a/b sets the energy scale. In terms of it and of the characteristic frequency of phonons $\omega_0 = \sqrt{v''(r_0)/m} = \sqrt{ab/m}$ of the system, we define the coupling parameter $g \equiv (\hbar\omega_0)/(2a/b) = (\hbar b^{\frac{1}{2}})/(2\sqrt{am})$, which rules the strength of the quantum effects. When $g \lesssim 1$ the LCA may be applied, and the effective nearest-neighbour potential is [46]

$$v_{\text{eff}}(r) = \frac{a}{b}\, e^{D_1 b^2/2}\, e^{-b(r-r_0)} + a(r - r_0) + B(T) + H(T). \tag{4.7}$$

$B(T)$ and $H(T)$ ($H(T)$ is the logarithmic term introduced in equation (3.13)) are constants depending only on temperature.

As the effective potential (4.7) has the same functional form as the original potential, the partition function, relevant thermodynamic quantities and correlation functions of the quantum system can be obtained *analytically* [46] in term of the Euler Γ-function and its derivatives, as in the classical system. Examples of the results obtained [46] are shown in figures 6 and 7 where the specific heat and the displacement correlation function of two neighbouring atoms are reported. Specific heat results reproduce those of the more cumbersome Bethe *ansatz* calculation, while the correlation function of the quantum Toda lattice appears as a result actually attainable only by the effective potential method.

By the same procedure as introduced for the Toda lattice, the LCA effective potential for a Morse interaction may be also constructed, and the thermodynamic quantities can be computed again analytically [47].

When more realistic potentials are used, one has to resort to numerical calculation. However [77], for one-dimensional systems with nearest-neighbour interaction this entails only the numerical solution of a nonlinear equation.

One of the most widely used interaction potentials in solid state and molecular physics is the Lennard-Jones potential:

$$v(r) = 4\varepsilon\left[(\sigma/r)^{12} - (\sigma/r)^{6}\right] \tag{4.8}$$

whose coupling parameter may be defined as $g = [(\hbar^2 v''(r_0))/(m\epsilon\sigma^2)]^{\frac{1}{2}}$, $r_0 = \sqrt[6]{2}\sigma$ being the classical equilibrium distance of nearest-neighbour atoms. The Lennard-Jones chain has been studied as a prototype model of three-dimensional rare gas solids, and both static and dynamical behaviour has been addressed, by Monte Carlo computation [126], molecular dynamics simulation [80] and effective potential [48, 78, 80, 82]. For such a potential, as for all the potentials not having a very simple analytical form like Toda, Morse or sine–Gordon (see the preceding subsection), the series given by the application of the operator Δ cannot be resummed in a closed form, and the LCA effective potential has to be taken in its original form (4.4). For ill-behaving potentials like Lennard-Jones, care must be taken with the series expansions of equation (4.4), as they have only asymptotic character, diverging

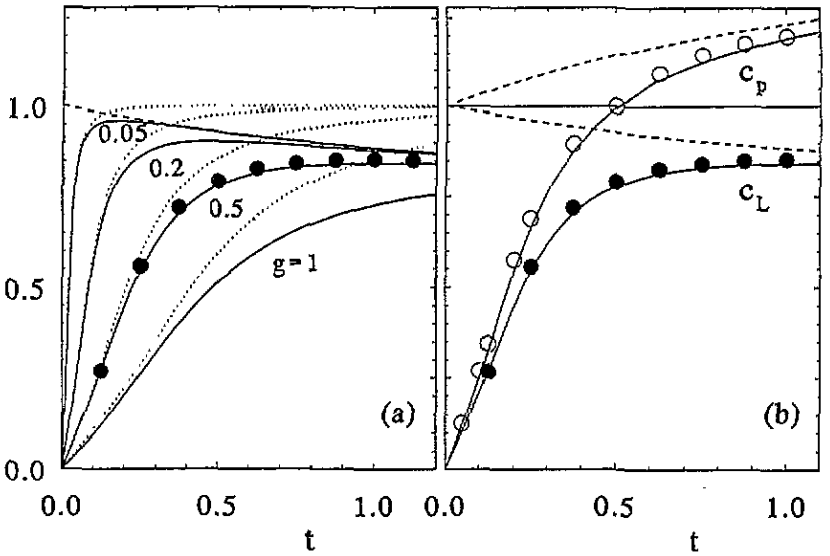

Figure 6. (a) Specific heat at constant length c_L as a function of t, for $d = r_0$ and different values of g (solid lines); the dotted lines give the corresponding curves in the self-consistent harmonic approximation, and the dashed line is the classical result ($g = 0$). The filled circles are the Bethe *ansatz* results by Hader and Mertens [123] for $g = 0.5$ (please note that in the paper by Hader and Mertens [123] a different definition of the reduced temperature is used, so that the reduced temperature of this figure, $t = k_B T b/2a$, differs by a factor of four from that of figures 7 and 8 of [123]). (b) Specific heat at constant length, c_L, for $d = r_0$, and at constant pressure, c_p, for $p = 0$, as a function of t for $g = 0.5$; the solid lines are the results of the variational method, the open and filled circles the Bethe *ansatz* results (cf. figure 7 of [123]) and the dashed lines the classical results.

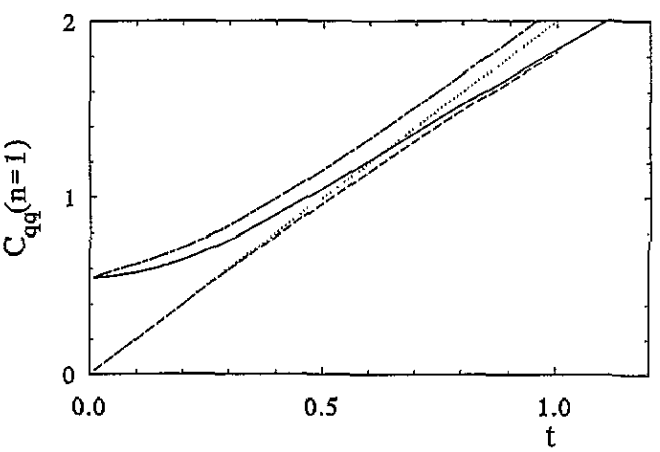

Figure 7. Position–position correlation function $C_{qq}(n = 1)$ [$C_{qq}(n) = \langle(\hat{q}_{i+n} - \hat{q}_i - nd)^2\rangle$] for g=0.5 versus the reduced temperature $t = k_B T b/2a$. The units of the y-axis are $1/b^2$. Solid line: quantum Toda chain; dash–dotted line: quantum harmonic chain; dashed line: classical Toda chain; dotted line: classical harmonic chain.

for any finite value of the renormalization parameter D_1. Despite this, when the LCA makes sense, only the very few first terms of the series are relevant, and reliable results may still be obtained. In figure 8 the internal energy and specific heat as given by the effective

potential [48] are reported for $g = 0.76$, a coupling which corresponds to the values of the Lennard-Jones parameters typical for neon, and compared with heavily computer-time consuming PIMC simulation results [126]. The good agreement between effective potential and PIMC data is not limited to macroscopic thermodynamic quantities, but is maintained also when more complicated static correlation functions are considered, as it will be shown in section 7.2 (figure 14).

4.3. Rare gas solids

In the previous sections we showed some applications of the effective potential method to simple zero- and one-dimensional quantum models, where full benefits result from the simplicity of the corresponding classical problem. However, the method displays all of its power also when it is subjected to the most stringent test for a physical theoretical device, i.e. when its ability to reproduce experimental data is probed. Indeed, the effective potential method has been successfully employed to describe the thermodynamic properties of rare gas solids at low and intermediate temperature [49, 50, 53, 52, 51, 54, 127, 11, 56, 59]. It is in the latter temperature region that it reveals itself to be particularly useful, as the other available theories, e.g. the SCHA and the ISC (improved self-consistent) methods, become rapidly no longer reliable when the temperature is not very low [50, 51, 11].

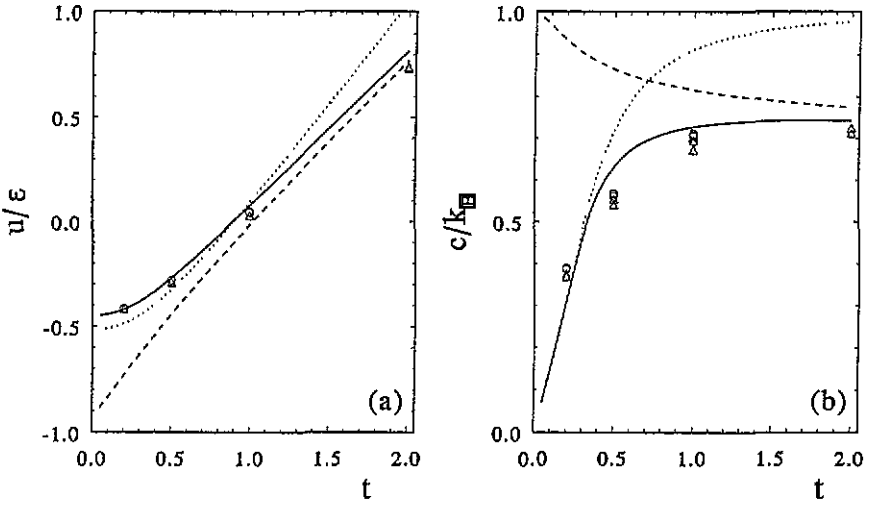

Figure 8. Equilibrium internal energy u and specific heat c per atom for the infinite Lennard-Jones chain and $g = 0.76$. Full line: results of the effective potential calculation; dotted line: harmonic approximation; dashed line: classical result; circles and triangles: quantum Monte-Carlo data from [126].

All the applications of the effective potential method to rare gas solids are based on its variant usually known as EPMC (effective potential Monte Carlo). Indeed, the definition and evaluation of the effective potential for a rare gas solid, modelled as a 3D array of atoms interacting by a pair-wise potential, closely resemble the procedure already described for the Lennard-Jones chain, apart from some technical modification due to the appearance of different phonon branches and the possible inclusion of interactions beyond the nearest neighbours. But the biggest difference between one- and three-dimensional systems is that, for the latter, the classical problem itself is not easy and can be afforded only numerically, i.e. by Monte Carlo simulations or molecular dynamics (MD) calculation. By the way, we

would like to remark that MD in conjunction with the effective potential may be safely used only to access quantum static averages, as there is no ground that the classical dynamics driven by the effective potential can constitute a good approximation of the true quantum dynamics of the system.

The numerous papers devoted to rare gas solids addressed different aspects of the problem, showing the effectiveness of EPMC; here we give only a sketch of the main results. For the heaviest rare gases (xenon, krypton and argon) the LCA at the lowest order already allows us to reproduce the experimental data for the specific heat and the equation of state, starting from the lowest accessible temperature up to the melting temperature; an example of the result obtained for argon using the Lennard-Jones potential (4.8) is shown in figure 9. When neon is considered the contribution coming from LCA highest-order terms becomes more important [50]; an improvement of EPMC which takes into account, in a perturbative way, also the renormalization effects of the cubic term of the expansion of the potential around the minimum, has been recently proposed [56], so that also at very low temperature EPMC is competitive, with respect to all other methods, in describing the thermal properties of solid neon.

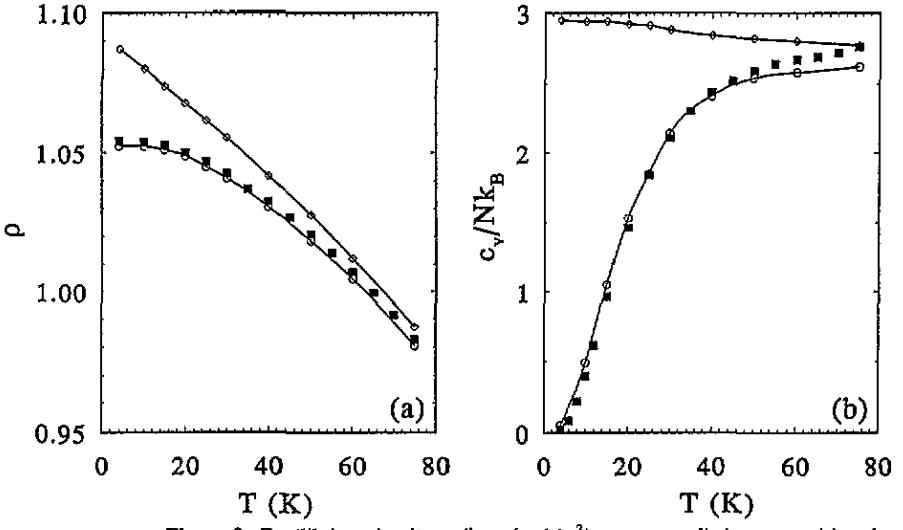

Figure 9. Equilibrium density ρ (in units $1/\sigma^3$) at zero applied pressure (a) and specific heat per atom c_v at constant volume (b) of solid argon. Open diamonds and full line through them: MC classical results; open circles and full line through them: EPMC quantum results [53]; filled squares: experimental data [128].

As already shown for the Lennard-Jones and Toda chains, EPMC allows us also to evaluate the quantum thermodynamic average of microscopic quantities. Among them, the kinetic energy per particle may be of interest, as has been directly measured in deep inelastic neutron scattering (DINS) experiments [129, 130]. The LCA expression for the kinetic energy per particle [54]

$$\langle \hat{K} \rangle = \frac{1}{2N}\sum_k \lambda_k + \frac{1}{2N}\sum_{|l-l'|=d}\left\{\left[\langle u''(x_{ll'})\rangle_G - u''(d)\right]\vartheta_L + \left[\left\langle\frac{u'(x_{ll'})}{x_{ll'}}\right\rangle_G - \frac{u'(d)}{d}\right]\vartheta_T\right\} \tag{4.9}$$

where

$$\vartheta_{\mathrm{L}} = \frac{1}{N}\sum_{k,\mu} 4\sin^2\frac{\boldsymbol{k}\cdot\boldsymbol{d}}{2}\left(\frac{\boldsymbol{d}\cdot\boldsymbol{\epsilon}_\mu(\boldsymbol{k})}{d}\right)^2 \frac{\hbar}{8m\omega_k}\left(\coth f_{k\mu} - \frac{f_{k\mu}}{\sinh^2 f_{k\mu}}\right) \tag{4.10}$$

$$\vartheta_{\mathrm{T}} = \frac{1}{N}\sum_{k,\mu} 4\sin^2\frac{\boldsymbol{k}\cdot\boldsymbol{d}}{2}\left[1-\left(\frac{\boldsymbol{d}\cdot\boldsymbol{\epsilon}_\mu(\boldsymbol{k})}{d}\right)^2\right] \frac{\hbar}{8m\omega_k}\left(\coth f_{k\mu} - \frac{f_{k\mu}}{\sinh^2 f_{k\mu}}\right) \tag{4.11}$$

clearly shows how the classical Gaussian distribution of momenta is modified by the quantum interplay between coordinates and conjugate momenta, which makes $\langle\hat{K}\rangle$ dependent on the interaction potential u between particles. Figure 10 shows the results obtained using the Lennard-Jones interaction potential, compared with some DINS experimental data. The agreement for argon may be considered very good, if we recall that the LJ potential is a crude approximation of the true potential, which should include multi-body effects.

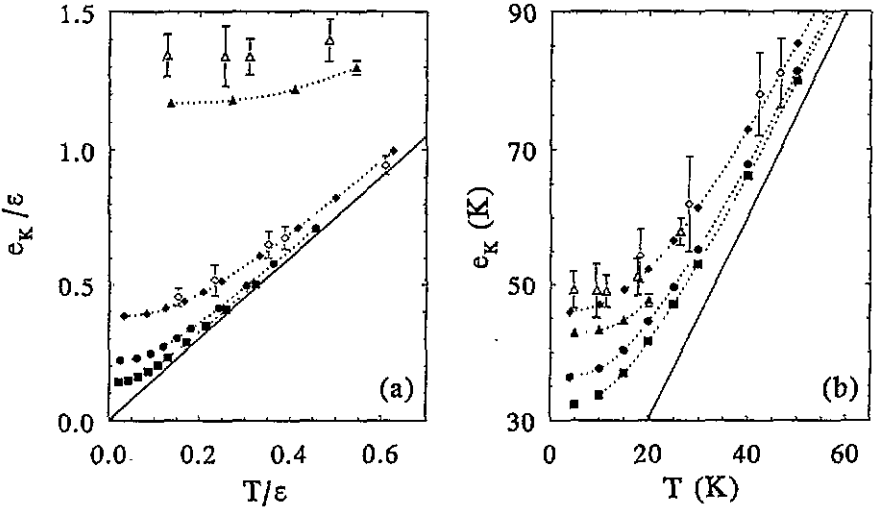

Figure 10. Kinetic energy per atom versus temperature [54]. Data for solid LJ neon (full triangles) were obtained by PIMC; data for argon (diamonds), krypton (circles), and xenon (squares) by EPMC. The solid line is the classical result $e_K = (3/2)T$, the open triangles are experimental data for neon [129], and open diamonds are experimental data for argon [130]. The scaling used in (a), where reduced units are used for both axes, gives a representation depending only on the coupling constant g. Plot (b), where dimensional units are employed, shows the quantum kinetic energies at low temperatures are comparable for different rare gases, in spite of the quite different quantum couplings.

A more complete discussion on the application of EPMC to rare gas solids, together with a comprehensive account of open problems for such systems and a comparison with other theoretical methods, may be found in the papers cited above, and especially in the review paper by Cowley and Horton [11].

5. Nonstandard systems

5.1. Phase-space path integral

In this section we briefly recall the expression of the Hamiltonian (or phase-space) path integral. Let us consider a quantum Hamiltonian $\hat{\mathcal{H}}(\hat{p},\hat{q})$ representing a system with M

degrees of freedom. The path integral giving the Weyl symbol (see section 3.3) for the quantum mechanical propagator $\exp[-i\hat{\mathcal{H}}(t_2 - t_1)]$ is derived and discussed in [105], and the path integral for the matrix elements $\rho(q'', q')$ can be obtained by performing the Wick rotation to the imaginary time $\beta = i(t_2 - t_1)$, and using equation (3.26), as shown in appendix E. The outcome is

$$\rho(q'', q') \equiv \langle q'' | \, e^{-\beta\hat{\mathcal{H}}} \, | q' \rangle = \int \mathcal{D}[p] \int_{q'}^{q''} \mathcal{D}[q] \; e^{S[p,q]}. \tag{5.1}$$

The limits on the integral imply that the sum is over all paths $\big(p(u), q(u)\big)$, $u \in [0, \beta]$, with the constraints $q(0) = q'$ and $q(\beta) = q''$. The action $S[p, q]$ is a local functional containing the Weyl symbol for $\hat{\mathcal{H}}$,

$$S[p, q] = \int_0^\beta du \; \big[ip^T(u)\dot{q}(u) - \mathcal{H}\big(p(u), q(u)\big)\big]. \tag{5.2}$$

For standard Hamiltonians (3.1) the momentum path integrals appearing in the above formulas can be explicitly evaluated, leaving Feynman's coordinate-only path integral, equations (3.2) and (3.3).

5.2. PQSCHA for nonstandard Hamiltonians

The derivation follows the same scheme of the standard case, section 3, so that we will comment only those parts that are peculiar to the nonstandard case. First, since we are dealing with a phase-space path integral (5.1), the average point of a path is given by

$$\frac{1}{\beta} \int_0^\beta du \, \big(p(u), q(u)\big) \tag{5.3}$$

so that (5.1) can equivalently be written as

$$\rho(q'', q') = \int d\bar{p} \, d\bar{q} \; \bar{\rho}(q'', q'; \bar{p}, \bar{q}) \tag{5.4}$$

where the reduced density

$$\bar{\rho}(q'', q'; \bar{p}, \bar{q}) = \int \mathcal{D}[p] \int_{q'}^{q''} \mathcal{D}[q] \, \delta \left[(\bar{p}, \bar{q}) - \frac{1}{\beta} \int_0^\beta du \, \big(p(u), q(u)\big) \right] e^{S[p,q]}. \tag{5.5}$$

collects the contributions from those paths with $(\bar{p}, \bar{q})$ as average point. In the place of the Weyl symbol $\mathcal{H}(p, q)$ we put, generalizing the trial potential (3.6), a trial function

$$\mathcal{H}_0(p, q; \bar{p}, \bar{q}) = w + \tfrac{1}{2} \delta p^T A^2 \delta p + \delta p^T X \, \delta q + \tfrac{1}{2} \delta q^T B^2 \delta q \tag{5.6}$$

where $\delta p \equiv p - \bar{p}$ and $\delta q \equiv q - \bar{q}$. Of course, the c-number w and the real $M \times M$ matrices $A^2 = \{A^2_{\mu\nu}\}$, $X = \{X_{\mu\nu}\}$ and $B^2 = \{B^2_{\mu\nu}\}$ are allowed to depend on $(\bar{p}, \bar{q})$, and are to be determined in order that $\bar{\rho}_0$, i.e. the path integral (5.5) with $\mathcal{H}_0$ instead of $\mathcal{H}$ in the action (5.2), at best approximates $\bar{\rho}$.

In order to reduce $\mathcal{H}_0$ to its normal form [131] we diagonalize the momentum part through the canonical transformation $(p, q) \to (A^{-1}p, Aq)$, and then introduce the orthogonal matrix $U(p, q) \equiv \{U_{k\mu}(p, q)\}$ that diagonalizes the coordinate part,

$$\sum\nolimits_{\mu\nu} U_{k\mu}(AB^2A)_{\mu\nu} U_{\ell\nu} = \delta_{k\ell} \left[\omega_k^2(\bar{p}, \bar{q}) + \sigma_k^2(\bar{p}, \bar{q})\right]. \tag{5.7}$$

Transforming the original canonical variables as

$$(p, q) \to (UA^{-1}p, UAq) \tag{5.8}$$

the matrix $\boldsymbol{X}$ in the mixed term becomes then $(\boldsymbol{U}\boldsymbol{A}^{-1}\boldsymbol{X}\boldsymbol{A}\boldsymbol{U}^{\mathrm{T}})_{k\ell} = \sigma_{k\ell}(\bar{p}, \bar{q})$; therefore, in order to decouple $\mathcal{H}_0$ as a sum of harmonic oscillators we must restrict the set of free parameters setting to zero the off diagonal elements of $\{\sigma_{k\ell}\}$, requiring

$$\left(\boldsymbol{U}\boldsymbol{A}^{-1}\boldsymbol{X}\boldsymbol{A}\boldsymbol{U}^{\mathrm{T}}\right)_{k\ell} = \delta_{k\ell}\,\sigma_k(\bar{p}, \bar{q}). \tag{5.9}$$

Note that with this choice $\mathcal{H}_0$ cannot exactly describe quadratic couplings that are non-harmonic, as the charged particle in a uniform magnetic field [132]. In practice, the independent parameters of $\mathcal{H}_0$ are replaced by the scalars ω_k^2 and σ_k, and by the independent components of the matrices $\boldsymbol{A}$ and $\boldsymbol{U}$.

The evaluation of the path integral for the reduced density $\bar{\rho}_0$ is reported in appendix F. The Weyl symbol for $\bar{\rho}_0$, equation (F.5), determines a Gaussian distribution in phase space, centred in $(\bar{p}, \bar{q})$, so that we use the pure quantum fluctuation variables (η, ξ) in the place of (p, q),

$$(p, q) \equiv (\bar{p} + \eta, \bar{q} + \xi). \tag{5.10}$$

Again, we *rub out the bar* over $\bar{p}$ and $\bar{q}$ and use the double-bracket notation for the Gaussian average determined by $\bar{\rho}_0$; its moments are $\langle\langle\eta\rangle\rangle = \langle\langle\xi\rangle\rangle = 0$ and, from equation (F.7),

$$\begin{aligned}
\langle\langle\eta_k\,\eta_\ell\rangle\rangle &= \delta_{k\ell}\left[\omega_k^2(p, q) + \sigma_k^2(p, q)\right]\alpha_k(p, q) \\
\langle\langle\eta_k\,\xi_\ell\rangle\rangle &= -\delta_{k\ell}\,\sigma_k(p, q)\,\alpha_k(p, q) \\
\langle\langle\xi_k\,\xi_\ell\rangle\rangle &= \delta_{k\ell}\,\alpha_k(p, q)
\end{aligned} \tag{5.11}$$

where $\eta_k = \{\boldsymbol{U}\boldsymbol{A}\eta\}_k$, $\xi_k = \{\boldsymbol{U}\boldsymbol{A}^{-1}\xi\}_k$, and

$$\alpha_k(p, q) = \frac{1}{2\omega_k(p, q)}\left(\coth f_k(p, q) - \frac{1}{f_k(p, q)}\right) \qquad f_k(p, q) = \tfrac{1}{2}\,\beta\omega_k(p, q). \tag{5.12}$$

It clearly appears that now, at variance with the standard case, the separation of the pure quantum fluctuations is made also for the momentum variables, and the cross-correlations are represented through the parameters σ_k. In the direct phase space, equations (5.11) correspond to the *renormalization parameters*

$$D_{\mu\nu}^{(pp)}(p, q) = \langle\langle\eta_\mu\eta_\nu\rangle\rangle \qquad D_{\mu\nu}^{(pq)}(p, q) = \langle\langle\eta_\mu\xi_\nu\rangle\rangle \qquad D_{\mu\nu}^{(qq)}(p, q) = \langle\langle\xi_\mu\xi_\nu\rangle\rangle. \tag{5.13}$$

Next, in analogy with equations (3.10) and (3.11), we impose the PQSCHA conditions in order to determine the parameters of $\mathcal{H}_0$. For w we have

$$w(p, q) = \left\langle\left\langle\mathcal{H}(p + \eta, q + \xi)\right\rangle\right\rangle - \sum\nolimits_k \omega_k^2(p, q)\,\alpha_k(p, q) \tag{5.14}$$

and for the matrices $\boldsymbol{A}^2$, $\boldsymbol{X}$, $\boldsymbol{B}^2$,

$$\begin{aligned}
A^2{}_{\mu\nu}(p, q) &= \left\langle\left\langle\partial_{p_\mu}\partial_{p_\nu}\mathcal{H}(p + \eta, q + \xi)\right\rangle\right\rangle \\
X_{\mu\nu}(p, q) &= \left\langle\left\langle\partial_{p_\mu}\partial_{q_\nu}\mathcal{H}(p + \eta, q + \xi)\right\rangle\right\rangle \\
B^2{}_{\mu\nu}(p, q) &= \left\langle\left\langle\partial_{q_\mu}\partial_{q_\nu}\mathcal{H}(p + \eta, q + \xi)\right\rangle\right\rangle.
\end{aligned} \tag{5.15}$$

Then we approximate the true density $\rho(q'', q')$ using $\bar{\rho}_0$ in equation (5.4). The associated Weyl symbol is found by integrating equation (F.5), and by (3.28) the expected classical-like expression for the average of an observable $\hat{O}(\hat{p}, \hat{q})$ follows:

$$\langle\hat{O}\rangle = \frac{1}{\mathcal{Z}}\int\frac{\mathrm{d}p\,\mathrm{d}q}{(2\pi)^M}\left\langle\left\langle\mathcal{O}(p + \eta, q + \xi)\right\rangle\right\rangle \mathrm{e}^{-\beta\mathcal{H}_{\mathrm{eff}}(p,q)} \tag{5.16}$$

with the effective Hamiltonian

$$\mathcal{H}_{\mathrm{eff}}(p, q) = w(p, q) + \frac{1}{\beta}\sum\nolimits_k \ln\frac{\sinh f_k(p, q)}{f_k(p, q)}. \tag{5.17}$$

In the standard case the above expressions reduce to the corresponding equations of section 3. In particular the matrix A^2 becomes constant and $X = \mathbf{0}$.

The differentiation operator (3.15) is naturally generalized in order to account for the momentum pure quantum renormalizations,

$$\Delta(p,q) \equiv \sum_{\mu\nu}\left[\tfrac{1}{2}D^{(pp)}_{\mu\nu}(p,q)\partial_{p_\mu}\partial_{p_\nu} + D^{(pq)}_{\mu\nu}(p,q)\,\partial_{p_\mu}\partial_{q_\nu} + \tfrac{1}{2}D^{(qq)}_{\mu\nu}(p,q)\partial_{q_\mu}\partial_{q_\nu}\right], \tag{5.18}$$

with the derivatives not operating on the D, so that

$$\left\langle\!\left\langle \mathcal{O}(p+\eta, q+\xi)\right\rangle\!\right\rangle \equiv e^{\Delta(p,q)}\,\mathcal{O}(p,q) \tag{5.19}$$

and using the obvious generalization of the identity (C.9) $\mathcal{H}_{\text{eff}}$ can be written in a form with a more evident renormalization part:

$$\mathcal{H}_{\text{eff}}(p,q) = \left[1-\Delta(p,q)\right]e^{\Delta(p,q)}\,\mathcal{H}(p,q) + \frac{1}{\beta}\sum_k \ln\frac{\sinh f_k(p,q)}{f_k(p,q)}. \tag{5.20}$$

Physically, equations (5.17) and (5.16) mean that the system tests its 'energy surface' only on the average over the neighbourhood of a phase-space point, and all observables are to be smoothed on the scale of the pure quantum fluctuations, which at $T = 0$ satisfy Heisenberg's uncertainty principle. Remarkably, as all pure quantum renormalizations are vanishing in the classical limit $f_k = \frac{1}{2}\beta\hbar\omega_k \to 0$, for high T we have $\mathcal{H}_{\text{eff}} \to \mathcal{H}$, so Weyl ordering appears to have a privileged role; this is not a bare consequence of our initial choice, as it can be verified that the PQSCHA gives Weyl symbols in the classical limit, even starting with different ordering rules. By construction this Hamiltonian PQSCHA formalism is exact when applied to harmonic Hamiltonians, and for standard systems it reduces to the effective potential method of section 3.

5.3. The low-coupling approximation

Solving the PQSCHA equations (5.15) and (5.11) is more involute than in the standard case, so the LCA is again in order. The reasoning made in section 3.2 is naturally generalized: namely, at low T the main contribution to the phase-space integral (5.16) arises from the neighbourhood of the minimum (p_0, q_0) of $\mathcal{H}_{\text{eff}}(p,q)$, and when T is raised, the renormalizations decrease and their dependence on (p,q) weakens as well. Following the procedure of section 3.2, we split the matrices (5.15) as

$$\begin{aligned} A^2(p,q) &= A^2 + \delta A^2(p,q) \\ X(p,q) &= X + \delta X(p,q) \\ B^2(p,q) &= B^2 + \delta B^2(p,q) \end{aligned} \tag{5.21}$$

(arguments of quantities taken in (p_0, q_0) are omitted) and we end up with the LCA effective Hamiltonian

$$\mathcal{H}_{\text{eff}}(p,q) = e^{\Delta}\,\mathcal{H}(p,q) - \Delta e^{\Delta}\,\mathcal{H}(p_0,q_0) + \frac{1}{\beta}\sum_k \ln\frac{\sinh f_k}{f_k} \tag{5.22}$$

and the minimum (p_0, q_0) is the solution of $(\partial_p, \partial_q)e^{\Delta}\mathcal{H}(p,q) = 0$.

For a *translation invariant* system with translation invariant (p_0, q_0) the matrix $U = U(p_0, q_0)$ is a Fourier transformation and $(UA^2U^{\mathrm{T}})_{k\ell} = m_k^{-1}\,\delta_{k\ell}$, so that

$$\begin{aligned} &\sum_{\mu\nu} U_{k\mu}U_{k\nu}e^{\Delta}\,\partial_{p_\mu}\partial_{p_\nu}\mathcal{H}(p_0,q_0) = m_k^{-1} \\ &\sum_{\mu\nu} U_{k\mu}U_{k\nu}e^{\Delta}\,\partial_{p_\mu}\partial_{q_\nu}\mathcal{H}(p_0,q_0) = \sigma_k \\ &\sum_{\mu\nu} U_{k\mu}U_{k\nu}e^{\Delta}\,\partial_{q_\mu}\partial_{q_\nu}\mathcal{H}(p_0,q_0) = m_k\left(\omega_k^2 + \sigma_k^2\right). \end{aligned} \tag{5.23}$$

It is useful in practice that the parameters m_k, σ_k and ω_k^2 appear as the coefficients of the harmonic approximation to $\mathcal{H}_{\text{eff}}$. In direct phase space the LCA renormalization parameters are then expressed as

$$\begin{aligned} D_{\mu\nu}^{(pp)} &= \sum_k U_{k\mu} U_{k\nu} m_k \left(\omega_k^2 + \sigma_k^2\right) \alpha_k \\ D_{\mu\nu}^{(pq)} &= -\sum_k U_{k\mu} U_{k\nu} \sigma_k \alpha_k \\ D_{\mu\nu}^{(qq)} &= \sum_k U_{k\mu} U_{k\nu} m_k^{-1} \alpha_k. \end{aligned} \tag{5.24}$$

The same conclusions as drawn in section 3.2 about the comparison with the SCHA are still valid here.

6. Nonstandard systems: applications

The aim of this section is to show how to apply the PQSCHA to magnetic systems: the main peculiarity of such systems is that, as they are described in terms of angular momentum operators, their Hamiltonians are intrinsically nonstandard.

The relevance of the PQSCHA is highlighted in this context, where semiclassical methods for standard systems cannot be used, unless one reduces the spin model to some canonical standard one, approximating or even cancelling out those terms of the Hamiltonian that make it non-standard, which usually means to renounce the description of the most interesting and peculiar nonlinear behaviours of magnets.

The ideal scheme to apply the PQSCHA is the following. First of all, as the method has been developed for canonical quantum Hamiltonians, the angular momentum operators have to be written in terms of canonical ones by means of a suitable spin-boson transformation. Once derived the $\hat{O}(\hat{p}, \hat{q})$ form of the operators corresponding to the interesting physical observables, the determination of their Weyl symbols is in order. The PQSCHA leads now to the evaluation of the renormalization coefficients appearing both in the effective Hamiltonian $\mathcal{H}_{\text{eff}}(p, q)$ and in all the other statistical averages. The inverse of the classical analogue of the spin-boson transformation used at the beginning, eventually leads to the effective spin Hamiltonian $\mathcal{H}_{\text{eff}}(s^x, s^y, s^z)$, s_i^x, s_i^y and s_i^z being now the three components of a classical unit vector sitting on site i.

This scheme is somewhat ideal in that some additional assumptions and approximations, depending on the specific system under investigation, have to be usually introduced on the way to the final result; in particular, both the quantum spin-boson transformation and the Weyl ordering have to be handled carefully, as they could hide subtle traps.

6.1. Easy-plane ferromagnetic chain

The PQSCHA has been first applied [72] to magnetic systems in order to study the thermodynamic properties of the *easy-plane ferromagnetic chain* (EPFC), described by the spin Hamiltonian

$$\hat{\mathcal{H}} = \sum_{i=1}^{N} \left[-J \hat{\boldsymbol{S}}_i \cdot \hat{\boldsymbol{S}}_{i+1} + D(\hat{S}_i^z)^2 - g_{\text{m}} \mu_{\text{B}} H \hat{S}_i^x \right] \tag{6.1}$$

where J and D are the exchange and anisotropy constants, g_{m} is the gyromagnetic ratio, H is an in-plane magnetic field and $\hat{\boldsymbol{S}}_i = \left(\hat{S}_i^x, \hat{S}_i^y, \hat{S}_i^z\right)$ are spin operators with $|\hat{\boldsymbol{S}}_i|^2 = S(S+1)$.

The EPFC is not only a 'toy model': there is a real compound, $CsNiF_3$, whose magnetic ions are arranged as chains in the lattice in such a way that the magnetic exchange coupling between the chains is very weak. Then, the behaviour is practically one dimensional (above

the 3D ordering temperature $T_N = 2.7$ K) and is described by the Hamiltonian (6.1), with $S = 1$, $J = 23.6$ K, $D = 9$ K, $g_m = 2.4$. One of the main reasons for this model to be the ideal candidate for the first application of the PQSCHA resides in the plentifulness of experimental, theoretical and numerical works available on it, that allow us to check the validity of the PQSCHA through an exhaustive comparison with previous results.

The 'easy-plane' character of the model suggests we make use, for each spin operator $\hat{S}$ (site index understood), of the quantum *Villain transformation* [133] to canonically conjugate operators $[\hat{\varphi}, \hat{S}^z] = \mathrm{i}$

$$\hat{S}^+(\hat{S}^z, \hat{\varphi}) = \mathrm{e}^{\mathrm{i}\hat{\varphi}}\sqrt{S(S+1) - \hat{S}^z(\hat{S}^z+1)} \qquad \hat{S}^-(\hat{S}^z, \hat{\varphi}) = (\hat{S}^+)^\dagger. \tag{6.2}$$

This transformation is sensible as long as $\langle \hat{S}^z \rangle < S$; if the temperature is not too high, this is ensured by the easy-plane anisotropy of the model. Note that, as $\hat{\varphi}$ represents the azimuthal angle, we prefer this notation in place of $\hat{q}$.

The transformed Hamiltonian is a relevant example of a nonstandard one, whose Weyl symbol, defining $\widetilde{S} \equiv S + \frac{1}{2}$ and the scaled momenta $\hat{p}_i = \hat{S}_i^z/\widetilde{S}$, turns out to be

$$\mathcal{H}(\boldsymbol{p}, \boldsymbol{\varphi}) = \varepsilon \sum_{i=1}^{N} \left[\frac{p_i^2}{2\gamma} - p_i p_{i+1} - \sqrt{(1-p_i^2)(1-p_{i+1}^2)}\cos(\varphi_i - \varphi_{i+1}) \right.$$
$$\left. - h\sqrt{1-p_i^2}\cos\varphi_i \right] \tag{6.3}$$

where $\varepsilon = J\widetilde{S}^2$, $h = g\mu_B H/(J\widetilde{S})$ and $\gamma = J/(2D)$; moreover we shall use in the following the *reduced temperature* $t = T/\varepsilon = T/(J\widetilde{S}^2)$. Note that disregarding anharmonic terms containing p_i leads to the *planar model*; and if one furthermore approximates $\cos(\varphi_i - \varphi_{i+1}) \sim 1 - (\varphi_i - \varphi_{i+1})^2/2$ the (modified) sine–Gordon model [41] is recovered.

The LCA and the symmetry properties of the model make equation (6.3) the only ingredient we need to write down the renormalizations coefficients

$$D_{ij}^{(pp)} = \frac{1}{2\widetilde{S}N}\sum_k \frac{b_k}{a_k}\left(\coth f_k - f_k^{-1}\right)\cos k(i-j)$$
$$D_{ij}^{(\varphi\varphi)} = \frac{1}{2\widetilde{S}N}\sum_k \frac{a_k}{b_k}\left(\coth f_k - f_k^{-1}\right)\cos k(i-j). \tag{6.4}$$

The self-consistent 'mass' and 'frequency' parameters m_k and ω_k enter the definition of the dimensionless quantities

$$a_k^2 \equiv \frac{1}{\varepsilon m_k} = \gamma^{-1} + \left[h\,\mathrm{e}^{-\frac{1}{2}\mathcal{D}_\parallel} + 2\,\mathrm{e}^{-\frac{1}{2}\mathcal{D}_\parallel} - 2(1-\cos k)\right]$$
$$b_k^2 \equiv \frac{m_k\omega_k^2}{\varepsilon} = h\,\theta^2\,\mathrm{e}^{-\frac{1}{2}\mathcal{D}_\parallel} + 2\theta^4\,\mathrm{e}^{-\frac{1}{2}\mathcal{D}_\parallel}(1-\cos k) \tag{6.5}$$

whose evaluation, being $f_k = a_k b_k/(2\widetilde{S}t)$, closes our self-consistent renormalization scheme. The coefficients (6.4) appear in the meaningful combinations $D_\perp \equiv D_{ll}^{(pp)}$, $D_\parallel \equiv D_{ii}^{(\varphi\varphi)}$, $\mathcal{D}_\parallel \equiv 2\left(D_{ll}^{(\varphi\varphi)} - D_{i,i+1}^{(\varphi\varphi)}\right)$ and $\theta^2 \equiv 1 - \frac{1}{2}D_\perp$.

After the effective Hamiltonian $\mathcal{H}_{\mathrm{eff}}(\boldsymbol{p}, \boldsymbol{\varphi})$ corresponding to equation (6.3) has been determined, the transformation

$$s_i^z = p_i/\theta \qquad s_i^x = \sqrt{1-(p_i/\theta)^2}\cos\varphi_i \qquad s_i^y = \sqrt{1-(p_i/\theta)^2}\sin\varphi_i \tag{6.6}$$

eventually leads to the effective classical spin Hamiltonian

$$\mathcal{H}_{\mathrm{eff}} = \varepsilon\theta^2\sum_i \left[-s_i^z s_{i+1}^z - \tau\left(s_i^x s_{i+1}^x + s_i^y s_{i+1}^y\right) + \frac{1}{2\gamma}\left(s_i^z\right)^2 - \tilde{h}\,s_i^x \right] + \varepsilon G(t) \tag{6.7}$$

$$G(t) = t\sum_k \ln \frac{\sinh f_k}{\theta f_k} - \frac{N}{2}\left[\left(2D_\perp + \theta^4 \mathcal{D}_\parallel\right)e^{-\frac{1}{2}\mathcal{D}_\parallel} + \tilde{h}\left(D_\perp + \theta^2 D_\parallel\right)\right] \tag{6.8}$$

where $s_i = (s_i^x, s_i^y, s_i^z)$ are now classical vectors of unit length $|s_i|^2 = 1$, while $\tilde{h} = h\,e^{-\frac{1}{2}\mathcal{D}_\parallel}$ and $\tau = \theta^2 e^{-\frac{1}{2}\mathcal{D}_\parallel}$.

Equation (6.7) shows a renormalization of the magnetic field ($h \to \tilde{h}$) and of the overall energy scale (by a factor of θ^2); an exchange anisotropy term (τ) appears as well; it accounts for the quantum enhancement of the out-of-plane fluctuations in competition against the easy-plane anisotropy. The quantum partition function is expressed, in terms of the effective Hamiltonian, as for a classical spin system

$$\mathcal{Z} = e^{-\beta F} = \int ds_1 \cdots ds_N \; e^{-\beta \mathcal{H}_{\text{eff}}(s_1,\ldots,s_N)} \tag{6.9}$$

where s_i varies on the unit sphere; in the one-dimensional case, integrals like the one appearing in equation (6.9) can be easily evaluated by means of the classical transfer-matrix method [134], so that, by means of equations (5.16) and (5.19) all the interesting thermodynamic averages can be studied. As an example we report in figure 11 the results for the 'excess' specific heat of $CsNiF_3$, i.e. the measured difference between the specific heat with and without applied field (the experimental measurements are particularly accurate since the lattice contribution is subtracted). This quantity generalizes the one reported in figure 5 for the sine–Gordon model, and is particularly sensitive to nonlinearity. The perfect agreement of the PQSCHA result with experiments comes from the solution of the problem in two aspects. Firstly, the 'classical counterpart' of the $S = 1$ spin chain is identified by the correspondence with a spin length $\tilde{S} = 3/2$ (and not unity, as in a naive approach), which is the correct model to start with in accounting for quantum effects; secondly, the nonlinearity in the out-of-plane variables is taken into account thanks to the Hamiltonian PQSCHA, and this gives quantitatively correct results, whereas the (standard) quantum planar model proves to be inadequate.

For the spin correlation functions, once one has determined the Weyl symbol for the operator product $\hat{S}_i^\mu \hat{S}_j^\mu$, evaluated the average $e^{\Delta} S_i^\mu S_j^\mu$ and reconstructed the spin variables following equations (6.6), one finally gets

$$\begin{aligned}
\left\langle \hat{S}_i^x \hat{S}_j^x \right\rangle &= \tilde{S}^2 \theta^4 e^{-D_\parallel}\left[\cosh D_{ij}^{(\varphi\varphi)} \langle s_i^x s_j^x\rangle_{\text{eff}} + \sinh D_{ij}^{(\varphi\varphi)} \langle s_i^y s_j^y\rangle_{\text{eff}}\right] r \\
\left\langle \hat{S}_i^y \hat{S}_j^y \right\rangle &= \tilde{S}^2 \theta^4 e^{-D_\parallel}\left[\cosh D_{ij}^{(\varphi\varphi)} \langle s_i^y s_j^y\rangle_{\text{eff}} + \sinh D_{ij}^{(\varphi\varphi)} \langle s_i^x s_j^x\rangle_{\text{eff}}\right] \\
\left\langle \hat{S}_i^z \hat{S}_j^z \right\rangle &= \tilde{S}^2\left(\theta^2 \langle s_i^z s_j^z\rangle_{\text{eff}} + D_{ij}^{(pp)}\right).
\end{aligned} \tag{6.10}$$

This holds for $i \neq j$. For $i = j$ the calculation has to be done more carefully, since it involves products of operators that are noncommuting, as they act on the same site.

6.2. Two-dimensional magnets

In the case of $CsNiF_3$ the comparison between results obtained by the PQSCHA and experimental and numerical simulation data leads to a very good agreement, as shown in figure 11 and figure 12; reasons for such a success have to be recognized in the peculiar way the PQSCHA allows us to take into account the nonlinear features of the model, meanwhile providing an exact description of the linear behaviour. This application gives us confidence to apply the method also in the two-dimensional case.

Nonlinear excitations, in fact, play a fundamental role also in two-dimensional magnets, and, in particular, in those systems whose *planar* character sustains the appearance of

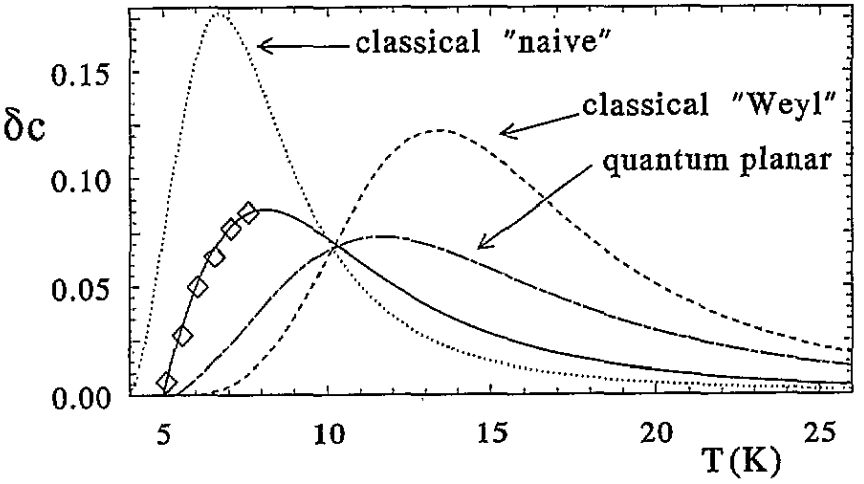

Figure 11. Excess specific heat per site $\delta c \equiv c(H) - c(0)$ of the quasi-one-dimensional $S = 1$ compound $CsNiF_3$ against temperature, at field $H = 5.8$ kG. Solid line: quantum EPFC; diamonds: experimental data from [135]. The dotted line refers to the classical counterpart of the Hamiltonian (6.1) taking a *naive* mapping of the spin operators onto vectors of length $\widetilde{S} = S$; the dashed line refers to $\widetilde{S} = S + 1/2$, and represents the meaningful classical limit given by the PQSCHA through Weyl ordering. The quantum planar approximated model (dash–dotted line) appears insufficient for a quantitative description.

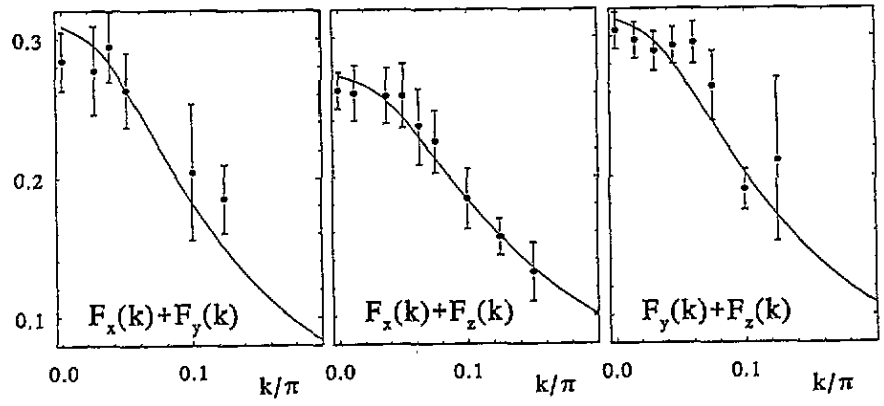

Figure 12. Combined components $F_x(k)$, $F_y(k)$ and $F_z(k)$ of the static structure factor of $CsNiF_3$, at field $H = 10$ kG and temperature $T = 12$ K. Solid line: quantum EPFC; circles: experimental data from [136]. Overall intensity scale determined by least-squares method.

vortices. The adjective *planar* refers to the appearance of an exchange anisotropy term that defines an easy plane for the spins, making energetically unfavourable their alignment along the direction perpendicular to that plane, as in the typical XXZ Hamiltonian

$$\hat{\mathcal{H}} = -\frac{1}{2} J \sum_{i,d} \left(\hat{S}_i^x \hat{S}_{i+d}^x + \hat{S}_i^y \hat{S}_{i+d}^y + \lambda \hat{S}_i^z \hat{S}_{i+d}^z \right) \tag{6.11}$$

where symbols have the same meaning as in the previous section and the index $i \equiv (i_1, i_2)$ runs over the sites of a two-dimensional Bravais lattice, $d \equiv (d_1, d_2)$ being the displacements of the z nearest neighbours of each site.

The class of models described by (6.11) with $0 \leqslant \lambda < 1$ has been recently studied

in relation to the Berezinskii-Kosterlitz-Thouless (BKT) transition. This in fact has been characterized for the *classical XY* model, i.e. the one in which the spins do not have z components at all. Note that this is an intrinsically classical model as in the quantum case out-of-plane fluctuations have to be considered, no matter what their explicit appearance in the Hamiltonian, $S_i^z \equiv 0$ being a physically meaningless constraint, basically because of the uncertainty principle.

The BKT transition is driven by the dissociation of vortex/antivortex pairs in the xy plane, a process that can be heavily affected by the possibility for the z components to be different from zero, demonstrated by the difficulties in deriving a clear picture of the quantum version of the subject. A good description of nonlinear excitations (vortices) and of quantum (out-of-plane) fluctuations is indeed the essential ingredient for such a picture to be drawn, and this indicates the PQSCHA as an ideal tool to further investigate the question.

The derivation of the effective Hamiltonian corresponding to equation (6.11) proceeds as in the one-dimensional case, leading to the explicit form

$$\mathcal{H}_{\text{eff}} = -\frac{\varepsilon}{2} j_{\text{eff}} \sum_{i,d} \left(s_i^x s_{i+d}^x + s_i^y s_{i+d}^y + \lambda_{\text{eff}} s_i^z s_{i+d}^z \right) + N\varepsilon\, G(t). \tag{6.12}$$

We see again that quantum effects renormalize the interaction parameters through $j \to j_{\text{eff}}$ and $\lambda \to \lambda_{\text{eff}}$, where

$$j_{\text{eff}}(t, S, \lambda) = \left(1 - \tfrac{1}{2} D_\perp\right)^2 \, \mathrm{e}^{-\frac{1}{2}\mathcal{D}_\parallel} \tag{6.13}$$

$$\lambda_{\text{eff}}(t, S, \lambda) = \lambda \, \left(1 - \tfrac{1}{2} D_\perp\right)^{-1} \, \mathrm{e}^{\frac{1}{2}\mathcal{D}_\parallel} \tag{6.14}$$

and the coefficients $D_\perp$ and $\mathcal{D}_\parallel$, as well as the additive term $G(t)$, have a form analogous to the one shown in the previous subsection.

The quantum fluctuations are responsible for a weakening of the easy-plane anisotropy ($\lambda_{\text{eff}} < \lambda$) and this could be a key point to understand the possible quantum version of the BKT transition. Let us then look at spin correlations on the easy plane: they turn out to be

$$\langle \hat{S}_i^x \hat{S}_j^x \rangle = \widetilde{S}^2 \left(1 - \tfrac{1}{2} D_\perp\right)^2 \mathrm{e}^{-\frac{1}{2}\mathcal{D}_\parallel} \, \exp\left(D_{ij}^{(\varphi\varphi)}\right) \langle s_i^x s_j^x \rangle_{\text{eff}}. \tag{6.15}$$

Since $D_{ij}^{(\varphi\varphi)}$ is bounded, the asymptotic behaviour of the correlations in the transition region is just the same as that of the effective classical model, so that the critical behaviour of the latter is preserved. It follows that the BKT temperature $t_c(S, \lambda)$ of the quantum system is connected with its classical counterpart $t_c^{(\text{cl})}(\lambda)$ by the self-consistent relation

$$\frac{t_c(S, \lambda)}{j_{\text{eff}}(t_c, S, \lambda)} = t_c^{(\text{cl})}\left(\lambda_{\text{eff}}(t_c, S, \lambda)\right). \tag{6.16}$$

Although the self-consistency of equation (6.16) is quite involute, due to the slight dependence of the classical critical temperature on λ, for $\lambda = 0$ we can easily determine the renormalized critical temperature; a graphical solution is shown in figure 13 where we have plotted, as functions of the reduced temperature t, the curve $j_{\text{eff}}(t, S, 0)$, for different values of the spin, and the line $t/t_c^{(\text{cl})}$, obtaining $t_c(S, 0)$ as the abscissae of the intersection points. The qualitative conclusion is that quantum effects lower the critical temperature and that this effect is stronger for smaller spins. From the quantitative point of view, since the transfer matrix method only applies to the one-dimensional case, the classical thermodynamic averages are to be calculated by numerical simulation [137], typically a Monte Carlo one. Nevertheless, the PQSCHA permits us to avoid much more complicated and computer time consuming quantum MC simulations; these become practically unaffordable for $S > \frac{1}{2}$, and in this case the approach by PQSCHA seems to be the only available one, making it an extremely interesting topic where much work can still be developed.

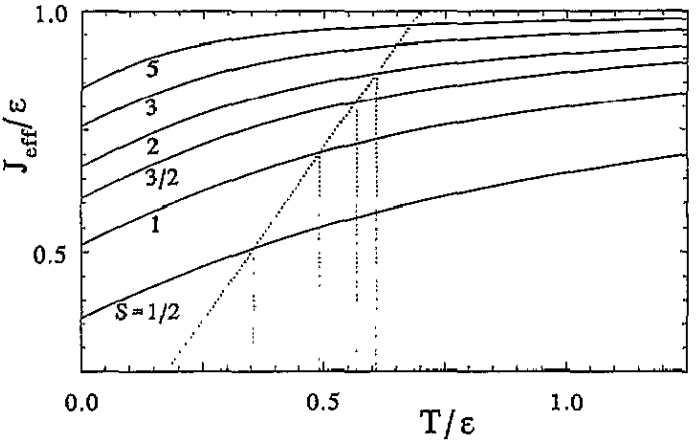

Figure 13. The effective exchange coupling $j_{\rm eff}(t, S, \lambda = 0)$ against temperature, for different values of S (solid lines). The energy unit is $\varepsilon = J\widetilde{S}^2 \equiv J(S + \frac{1}{2})^2$. The slope of the dotted line is the inverse of the classical BKT critical temperature from [137]. The abscissae of the intersection points give the expected quantum BKT transition temperatures.

The classical transition temperature for $\lambda = 0$ is found to be [137] $t_{\rm c}^{\rm (cl)} = 0.70 \pm 0.01$, and in the extreme case of $S = \frac{1}{2}$ our solution for its quantum counterpart is $t_{\rm c}(\frac{1}{2}, 0) \simeq 0.35$, in fair agreement with the quantum Monte Carlo result [138] (0.353 ± 0.003).

7. Dynamics with the PQSCHA

7.1. Approaches to dynamics

Dynamic correlations play an important role in condensed matter physics. In general, we are interested in time dependent correlation functions like

$$\langle \hat{\mathcal{O}}_1(t)\, \hat{\mathcal{O}}_2 \rangle = \mathrm{Tr}\left(\mathrm{e}^{-\beta\mathcal{H}}\, \mathrm{e}^{-\mathrm{i}\hat{\mathcal{H}}t}\, \hat{\mathcal{O}}_1\, \mathrm{e}^{\mathrm{i}\hat{\mathcal{H}}t}\, \hat{\mathcal{O}}_2 \right). \tag{7.1}$$

Without loss of generality we assume $\langle \hat{\mathcal{O}}_1 \rangle = \langle \hat{\mathcal{O}}_2 \rangle = 0$. The time Fourier transform of this correlation function is related to the spectral line-shape as probed by many experimental techniques like NMR, EPR, neutron scattering, etc. There are many methods to approach these functions. For the classical case molecular dynamics (MD) represents one of the most powerful numerical methods. In the quantum case the problem is still open when one wishes to go beyond perturbative many-body approaches; only recently very important exact results have been obtained for some one-dimensional systems [139]. The numerical results are confined to the analytic continuation of quantum Monte Carlo data, which is rather cumbersome and presents accuracy problems. The effective potential can give new ideas to approach the problem. We will treat in detail the method based on the frequency moment expansion, while we will give here only an outline of the so called *centroid molecular dynamics*, recently introduced [86, 88, 89].

Let us consider here for simplicity the autocorrelation function $\langle \hat{\mathcal{O}}(t)\, \hat{\mathcal{O}} \rangle$ of a Hermitian observable $\hat{\mathcal{O}} = \hat{\mathcal{O}}^\dagger$. In this case, it turns out to be more useful to deal with the 'symmetrized' correlation:

$$C(t) = \tfrac{1}{2}\left[\langle \hat{\mathcal{O}}(t)\, \hat{\mathcal{O}} \rangle + \langle \hat{\mathcal{O}}(-t)\, \hat{\mathcal{O}} \rangle \right] \tag{7.2}$$

which is a real and even function of time. Its Fourier transform $C(\omega)$ is real and even as well, in the frequency domain.

In order to take into account the quantum effects related to the noncommutativity of the operators and the detailed balance factor, Kubo [140] introduced the relaxation function

$$R(t) = \frac{1}{\beta}\int_0^\beta d\lambda \left\langle \hat{O}(0)\,\hat{O}(t + i\hbar\lambda)\right\rangle \tag{7.3}$$

whose Fourier transform $R(\omega)$ is related to $C(\omega)$ through the spectral theorem:

$$C(\omega) = \frac{\hbar\omega}{2}\coth\frac{\beta\hbar\omega}{2}\,R(\omega). \tag{7.4}$$

Mathematically, correct moment expansions have been proposed for both correlation and relaxation functions [84, 85]. In the following we refer to $C(t)$ and $C(\omega)$, even though the Mori [83, 84, 141] approach based on the relaxation function gives a more precise physical insight when approximations are requested [142, 143, 144]. However, all moments are in principle accessible for $C(\omega)$, while the zeroth moment of $R(\omega)$ cannot be exactly obtained. Taking into account that the odd moments are vanishing, let us define

$$\mu_{2n} = \int_{-\infty}^{+\infty} d\omega\, \omega^{2n} C(\omega) \tag{7.5}$$

so that the short-time behaviour of $C(t)$ is:

$$C(t) = \frac{1}{2\pi}\left(\mu_0 - \tfrac{1}{2}\mu_2 t^2 + \tfrac{1}{24}\mu_4 t^4 - \cdots\right). \tag{7.6}$$

The moments turn out to be expressed by equilibrium averages containing an increasing number of operators, deriving from multiple commutators with the Hamiltonian.

$$\mu_{2n} = 2\pi i^{2n}\left\langle [\hat{\mathcal{H}}, [\hat{\mathcal{H}}, \ldots, [\hat{\mathcal{H}}, \hat{O}]\cdots]]\,\hat{O}\right\rangle \qquad (2n \text{ commutators}). \tag{7.7}$$

These quantities can indeed be evaluated by means of the effective Hamiltonian or effective potential. However the *naive* moment expansion is very poorly convergent. It has been proved that only the short-time behaviour can be described by means of a reasonable number of moments.

Starting from the knowledge of the frequency moments, a reconstruction of the function $C(k, \omega)$ has been devised by Mori and Dupuis [83, 84, 85] by means of the continued fraction expansion. It can be proven that the correlation function can be written as $C(\omega) = (\mu_0/\pi)\,\mathrm{Re}[\psi_0(i\omega)]$, where the function ψ_0 of the complex variable z admits the following continued fraction representation:

$$\psi_n(z) = \cfrac{1}{z + \delta_{n+1}\psi_{n+1}(z)}. \tag{7.8}$$

In the time domain, $\psi_n(t)$ is called the nth memory function, and the coefficients δ_n are related to the frequency moments [84]. The explicit expressions for the first three are

$$\delta_1 = \frac{\mu_2}{\mu_0} \qquad \delta_2 = \frac{\mu_4}{\mu_2} - \frac{\mu_2}{\mu_0} \qquad \delta_3 = \frac{1}{\delta_2}\left[\frac{\mu_6}{\mu_2} - \left(\frac{\mu_4}{\mu_2}\right)^2\right]. \tag{7.9}$$

For a harmonic system δ_n vanishes for $n > 1$. In general, the continued fraction must be truncated at a certain level, because, when the order of moments increases, their numerical calculation becomes more and more cumbersome and, at the same time, a higher precision is required to maintain the relative error on the δ parameters reasonably small. Nevertheless, the knowledge of the first δ parameters allows us to reproduce a correlation function which,

in contrast with the simple moment expansion (7.6), joins the exact short-time behaviour with a well behaved long-time tail.

In order to calculate the spectral shape for anharmonic systems, we must thus resort to a reasonable approximation of the nth memory function [145] for n larger than some n_0, a procedure called *termination* of the continued fraction. However, the choice of the termination is a source of arbitrariness, it being generally related to the unknown long-time behaviour of the correlations, which cannot be guessed from the knowledge of the first moments. Unless some insight into the behaviour of the dynamic variables of the system may be obtained, the reconstruction of the spectral shapes of strongly anharmonic systems may thus suffer from poor control on the validity of the approximations employed [146, 147].

We suggested [80] obtaining such an insight from the MD data for the classical counterpart of the system. Namely, one constructs the classical spectra with the available classical moments and the termination of the continued fraction is chosen in such a way to reproduce as well as possible the MD reference data. Then one replaces the classical moments with the quantum ones keeping the same (classical) termination. This approximation is based on the assumption that long times, which are associated with low frequencies, are less affected by quantum fluctuations. This is also in the spirit of the recurrence method [148], with the classical MD spectra as reference.

Very recently, a different approach to quantum dynamical correlations was proposed [86, 88, 89] starting from equation (2.28). Here we simply describe the general idea; the method is largely discussed by the authors, also in their review paper [12]. Firstly, a generalization of the equation (2.28) was presented for two operators at different imaginary times, within a first-order cumulant approximation. Successively, an analytic continuation has been done; in this way the quantum detailed balance factor is recovered. Secondly, the observation that equation (2.28) represents an ergodic system whose potential is V_{eff} leads the authors to construct a 'centroid molecular dynamics' of quantities containing the quantum Gaussian fluctuations. In this way the 'centroid' $q_c(t)$ (its definition coincides with that of average point) evolves by means of a classical-like dynamics, under a force obtained by averaging with the Gaussian fluctuations, while the quantity of interest is itself fluctuating around $q_c(t)$ with the Gaussian pure quantum recipe. The comparison with the evolution equation for the Kubo relaxation function [140] of position operators shows that the method reproduces the correct expansion up to t^2 (i.e. the second moment) while the long-time behaviour is practically the classical one. Preliminary results have been recently published, all referring to systems where either the anharmonicity or the quantum effects are very small. It would be interesting to test this approach for many-body systems in the region of temperatures where both quantum effects and anharmonicity are relevant.

7.2. Dynamical response by frequency moments

The effective potential method has been employed to calculate the first even quantum moments for the Lennard-Jones chain [78], the Toda lattice [81] and recently also for a model of solid argon [79]; from the knowledge of moments, by using the continued fraction representation and applying suitable termination schemes, the spectral shape has been reconstructed. For the Lennard-Jones chain and the Toda lattice the correlation function

$$C(k,\omega) = \frac{1}{N}\sum_{ij} \mathrm{e}^{-\mathrm{i}kd(i-j)} \int \mathrm{d}t\ \mathrm{e}^{\mathrm{i}\omega t} \left\langle \left(\hat{u}_i(t) - \hat{u}_j(0)\right)^2 \right\rangle \tag{7.10}$$

has been considered, where $\hat{u}_i(t)$ is the displacement of the the ith atom from its equilibrium position.

As shown in [78, 81], explicit expressions for the even frequency moments of $C(k, \omega)$ can be obtained in terms of integrals like

$$\int_{-\infty}^{\infty} \mathrm{d}r \; v^{(n)}(r) v^{(m)}(r) \mathrm{e}^{-s_0 r - \beta v_{\mathrm{eff}}(r)} \tag{7.11}$$

where $v^{(n)}(r)$ denotes the nth derivative of the nearest-neighbour interaction potential $v(r)$ with respect to its argument, and $v_{\mathrm{eff}}(r)$ is its renormalized form as defined in section 4.2.

In [78] the moments for the Lennard-Jones chain, up to the fourth one, were computed also by PIMC simulation. An example of the comparison between the effective potential method and PIMC data is shown in figure 14 for the zone-boundary wave-vector $k = \pi/d$, d being the lattice spacing; the agreement is very good, but when dealing with dynamics we must remember that even small errors on the moments may give large errors in the expansion parameter δ_n of the continued fraction, so that the statistical errors of PIMC data may produce drastic modifications of the line-shapes.

Sample spectral shapes at half of the zone boundary for the quantum Lennard-Jones chain are shown in figure 15; they were obtained by a four-pole termination [149] of the continued fraction, using for the termination parameter $\tau_4^{-1} \equiv \delta_4 \psi_4(z) \simeq$ constant the value obtained from the fitting of molecular dynamics data for the classical system; it is worthwhile to observe that at the zone boundary the fitting procedure gives essentially the same results which may be found by a second-order Gaussian termination [150, 142] using only the calculated moments.

Following the same scheme, work is in progress for approaching the spectral shape of Lennard-Jones three-dimensional rare gas solids [79].

When the Toda lattice is considered, we have again the big advantage that the integrals (7.11) can be computed analytically; this allowed the authors of [81] to easily evaluate classical moments up to the eighth one, and to check the reliability of termination schemes for such a system by looking at the stability of the line-shape when the truncation is shifted to higher order.

The soft-mode behaviour in a one-dimensional model ferroelectric has also been recently investigated by the effective potential method [55].

8. Conclusions and perspectives

According to a more general point of view, we have presented a tutorial derivation of the effective potential and effective Hamiltonian approach to quantum effects in condensed matter physics. Several applications in different fields show the power of the method whenever the quantum character of the system is substantially related to the quadratic part of the Hamiltonian so that quantum fluctuations can be treated separately, in the one-loop (Gaussian) approximation. The classical nonlinearity is fully considered since Feynman's path integral allows the separation of the fluctuations into their classical and pure quantum parts, and the latter only can be independently approximated in the spirit of the self-consistent harmonic approximation (SCHA), a procedure that we have called the *pure quantum* SCHA (PQSCHA).

The main advantages of the PQSCHA are (a) in the unified description of quantum thermodynamics in the whole temperature range, since the almost-harmonic low-T behaviour and the correct quasi-classical high-T behaviour are simultaneously accounted for, and (b) in the simplicity of its implementation in terms of classical-like thermal averages with

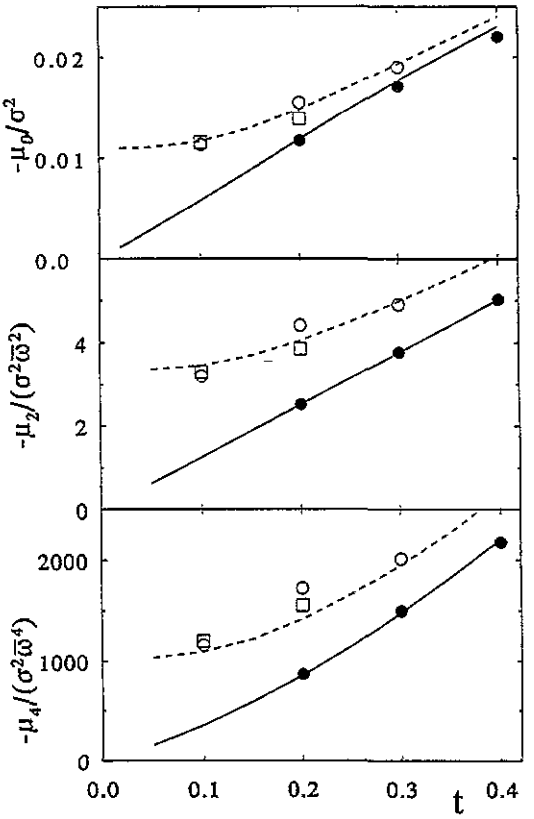

Figure 14. Moments μ_0, μ_2 and μ_4 for $kd = \pi$ versus the reduced temperature $t = k_B T/\varepsilon$; $\overline{\omega} = \sqrt{\varepsilon/m\sigma^2}$. The solid line is the classical result, the dashed line the quantum effective potential result, while the symbols are the classical and quantum Monte Carlo data. The quantum results refer to $g = 0.23$, the quantum coupling typical of argon. The classical MC data (filled circles) are those obtained for a chain of 40 atoms, while the QMC data are the results for a chain of 20 atoms (open circles) and 40 atoms (open squares). μ_0 is measured in units σ^2, μ_2 in units $\sigma^2\overline{\omega}^2$ and μ_4 in units $\sigma^2\overline{\omega}^4$.

an effective potential or Hamiltonian. Therefore, the PQSCHA is particularly powerful in the study of quantum properties at intermediate temperatures, especially when the nonlinearity yields a peculiar behaviour also in the classical limit, such as for those systems supporting nonlinear excitations like solitons or vortices. In the zero-dimensional case (one degree of freedom), the method permits us to take into account the change of symmetry of the effective potential due to the quantum effects in order to determine a ground state different from the classical one, the PQSCHA being at $T = 0$ equivalent to the SCHA.

Recently, the approach has been improved [151] for taking into account higher-order pure quantum contributions, extending Feynman's variational principle to higher-order terms of the cumulant expansion. Nonperturbative effects like quantum tunnelling need to be inserted *ad hoc*. However, we notice that these effects are not relevant for the statistical mechanics except at lowest temperatures.

In the multi-dimensional case, the full self-consistent approach looks formidable and a further approximation (LCA) is in general necessary for realistic calculations, even though some progress has been recently made [56]. In one space dimension the method shows all

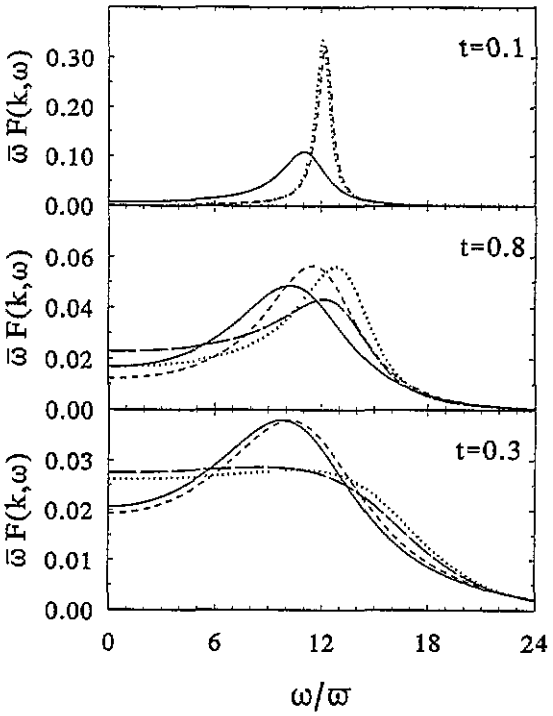

Figure 15. Classical and quantum relaxation function $F(k, \omega)$ at $kd = 0.5\pi$ and three different reduced temperatures $t = k_B T/\epsilon$. $\bar{\omega} = \sqrt{\epsilon/m\sigma^2}$ is the characteristic frequency scale of the Lennard-Jones chain. The continuous and dashed lines are the classical and quantum results, respectively, as given by a second-order Gaussian termination; the long-dashed and dotted lines are the classical and quantum four-pole relaxation function, respectively, obtained by using the value of τ_4 deduced from the fitting of the classical MD data [80].

of its power: reducing quantum calculations to a classical transfer matrix is very gratifying. The comparisons with available exact results have assured its reliability.

For three-dimensional systems, numerical simulations are always necessary, and some authors [127, 152] have discussed the convenience of the method with respect to the usual path integral Monte Carlo (PIMC). The first objection refers to the presence of quantum anharmonic effects on the ground state [153, 152]. Indeed, such effects were successfully accounted for in a recent paper [56]. The other (more pertinent) objection concerns the approximate nature of the effective potential with respect to the (in principle) exact PIMC approach. However, we point out that the exact PIMC results are found in the limit of infinite Trotter number: increasing it leads to an increase of the computer time needed and of the final numerical uncertainty. Even for small quantum coupling, one often needs a high Trotter number just to recover the quantum harmonic oscillator behaviour [67]. This shortcoming has stimulated the search for improved high-T approximations of the density matrix [154, 155, 156, 66] in order to embody the harmonic behaviour in the high-temperature approximation of the density matrix that enters the fundamental PIMC formula.

A complementary point of view involves the possibility of considering the Matsubara decomposition of the path integral, accounting for a finite number of Matsubara frequencies [157, 64]; however, the theoretical interest of such approaches is greater than their usefulness in numerical simulations, given the need for time consuming Fourier transformation routines at any MC step.

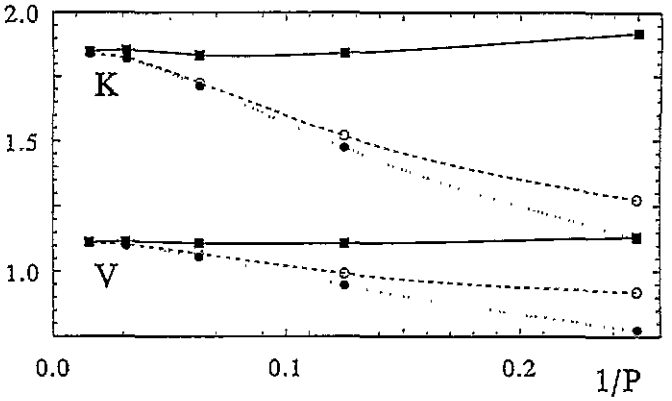

Figure 16. Extrapolation in the Trotter number P of the PIMC values for kinetic energy K and potential energy V for the one-dimensional lattice with Morse interaction, $v(x) = (e^{-x} - 1)^2$. The coupling is $g = 3.1$ (obtained as in (2.37) from characteristic interaction parameters for helium atoms) and the temperature $T = \varepsilon \sim 10$ K. Closed circles: raw PIMC outcomes; open circles: HA corrected data; squares: SCHA correction as proposed in [67].

However, the PQSCHA method can also be used to construct a better PIMC action, improving the afore-mentioned attempts. A first simple but effective step in this direction was the proposal of correcting the raw PIMC outcomes in the spirit of the SCHA [67]: in figure 16 the resulting improved extrapolation in the Trotter number is apparent and represents an interesting perspective for the numerical simulation of quantum solid state systems. Further work is in progress along this line.

Acknowledgment

The fruitful collaboration with A A Maradudin, A R McGurn, A Macchi and G Pedrolli is gratefully acknowledged. We would like also to thank W Janke and H Kleinert, J Cao and G A Voth and G K Horton and E R Cowley for discussions and for keeping us informed of their work. During the preparation of this work VT and RV have benefitted of the hospitality of S W Lovesey at the ISIS facilities.

Appendix A. Thermodynamics of the harmonic oscillator

The main tools used in this paper are the well known results for the harmonic oscillator with frequency ω, i.e. $V(\hat{q}) = m\omega^2\hat{q}^2/2$, that we report here for convenience. Its quantum density matrix at the equilibrium temperature $T = \beta^{-1}$ reads

$$\rho^{(h)}(q'', q'; \omega) = \sqrt{\frac{m\omega}{2\pi\hbar \sinh 2f}} \exp\left\{-\frac{m\omega}{4\hbar}\left[(q''+q')^2 \tanh f + (q''-q')^2 \coth f\right]\right\} \quad \text{(A.1)}$$

where $f = f(\omega) = \beta\hbar\omega/2$. The configuration density turns out to be a Gaussian,

$$\rho^{(h)}(q; \omega) \equiv \rho^{(h)}(q, q; \omega) = \frac{1}{2\sinh f} \frac{1}{\sqrt{2\pi\alpha_Q}} e^{-q^2/2\alpha_Q} \quad \text{(A.2)}$$

with variance $\alpha_Q = \alpha_Q(\omega) = (\hbar/2m\omega)\coth f(\omega)$, and the partition function is $\mathcal{Z}_Q^{(h)}(\omega) = (2\sinh f)^{-1}$, so that the free energy is $F_Q^{(h)}(\omega) = \beta^{-1}\ln(2\sinh f)$.

The classical limit is obtained for $f(\omega) \to 0$, and we have again a Gaussian configuration density, but with $\alpha_C = \alpha_C(\omega) = \hbar/\big(2m\omega f(\omega)\big) = 1/(m\beta\omega^2)$, and the partition function and the free energy become $\mathcal{Z}_C^{(\mathrm{h})}(\omega) = (2f)^{-1}$ and $F_C^{(\mathrm{h})}(\omega) = \beta^{-1}\ln(2f)$, respectively.

Appendix B. Standard PQSCHA: one degree of freedom

In equation (2.21) consider the action

$$S_0[q(u)] = -\frac{1}{\hbar}\int_0^{\beta\hbar} \mathrm{d}u\left[\tfrac{1}{2}m\dot{q}^2(u) + V_0\big(q(u);\bar{q}\big)\right] \tag{B.1}$$

with V_0 given by (2.23). Let us consider here the whole density matrix $\rho(q'',q') = \langle q''|\,\mathrm{e}^{-\beta\hat{\mathcal{H}}}\,|q'\rangle$ and the associated reduced density matrix $\bar{\rho}_0(q'',q';\bar{q})$. We obtain

$$\begin{aligned}\bar{\rho}_0(q'',q';\bar{q}) &= \int_{q'}^{q''}\mathcal{D}[q]\;\delta\left(\bar{q} - \frac{1}{\beta\hbar}\int_0^{\beta\hbar}\mathrm{d}u\,q(u)\right)\,\mathrm{e}^{S_0[q(u)]}\\ &= \frac{\beta}{2\pi}\int\mathrm{d}y\int_{q'}^{q''}\mathcal{D}[q]\;\exp\left(S_0[q(u)] + \frac{1}{\hbar}\int_0^{\beta\hbar}\mathrm{d}u\left[\mathrm{i}y\big(\bar{q}-q(u)\big)\right]\right)\\ &\equiv \frac{\beta}{2\pi}\int\mathrm{d}y\;\rho_1(q'',q';\bar{q};y).\end{aligned} \tag{B.2}$$

The integral over the variable y comes from the Fourier representation of Dirac's δ function. Now, $\rho_1(q'',q';\bar{q};y)$ is nothing but the density matrix corresponding to the harmonic Hamiltonian

$$\begin{aligned}\hat{\mathcal{H}}_1 &= \frac{\hat{p}^2}{2m} + w + \frac{m\omega^2}{2}(\hat{q}-\bar{q})^2 + \mathrm{i}y(\hat{q}-\bar{q})\\ &= w + \frac{y^2}{2m\omega^2} + \frac{\hat{p}^2}{2m} + \frac{m\omega^2}{2}\left(\hat{q}-\bar{q}+\frac{\mathrm{i}y}{m\omega^2}\right)^2.\end{aligned} \tag{B.3}$$

Therefore we can immediately use the (analytic continuation of) equation (A.1) and, transforming for convenience the dummy variable $y \to m\omega^2 y$ we obtain

$$\begin{aligned}\bar{\rho}_0(q'',q';\bar{q}) &= \frac{\beta m\omega^2}{2\pi}\,\mathrm{e}^{-\beta w}\int\mathrm{d}y\;\mathrm{e}^{-\frac{1}{2}\beta m\omega^2 y^2}\;\rho^{(\mathrm{b})}(q''-\bar{q}+\mathrm{i}y, q'-\bar{q}+\mathrm{i}y;\omega)\\ &= \frac{m\omega f}{\pi\hbar}\,\mathrm{e}^{-\beta w}\sqrt{\frac{m\omega}{2\pi\hbar\sinh 2f}}\\ &\quad\times\int\mathrm{d}y\;\exp\left(-\frac{m\omega}{\hbar}\Big[fy^2 + (\xi+\mathrm{i}y)^2\tanh f + \frac{1}{4}(q''-q')^2\coth f\Big]\right)\\ &= \sqrt{\frac{m}{2\pi\hbar^2\beta}}\,\mathrm{e}^{-\beta w}\,\frac{f}{\sinh f}\,\frac{1}{\sqrt{2\pi\alpha}}\exp\left(-\frac{\xi^2}{2\alpha} - \frac{m\omega\coth f}{4\hbar}(q''-q')^2\right)\end{aligned} \tag{B.4}$$

where $\xi = (q''+q')/2 - \bar{q}$ $f = \beta\hbar\omega/2$ and $\alpha = \alpha(\bar{q})$ is the parameter given by (2.25). The corresponding reduced configuration density $\bar{\rho}_0(q;\bar{q}) \equiv \bar{\rho}(q,q;\bar{q})$ takes then the form (2.24).

Appendix C. Standard PQSCHA: many degrees of freedom

In the definition (3.4) consider the trial action ($\hbar = 1$)

$$S_0[q(u)] = -\int_0^{\beta}\mathrm{d}u\left[\tfrac{1}{2}\,\dot{q}^{\mathrm{T}}(u)A^{-2}\dot{q}(u) + V_0(q;\bar{q})\right] \tag{C.1}$$

where V_0 is given by equation (3.6), and introduce the Fourier representation of the delta function. The trial reduced density then reads

$$\tilde{\rho}_0(q'', q'; \bar{q}) = \left(\frac{\beta}{2\pi}\right)^M \int \mathrm{d}y \int_{q'}^{q''} \mathcal{D}[q]\ \exp\left(S_0[q(u)] + \int_0^\beta \mathrm{d}u\ [\mathrm{i}y^{\mathrm{T}}(\bar{q} - q(u))]\right)$$
$$\equiv \left(\frac{\beta}{2\pi}\right)^M \int \mathrm{d}y\ \rho_1(q'', q'; \bar{q}; y). \tag{C.2}$$

Here, $\rho_1(q'', q'; \bar{q}; y)$ is the density matrix corresponding to the harmonic Hamiltonian

$$\hat{\mathcal{H}}_1 = \tfrac{1}{2}\hat{p}^{\mathrm{T}}A^2\hat{p} + w + \tfrac{1}{2}(\hat{q} - \bar{q})^{\mathrm{T}}B^2(\hat{q} - \bar{q}) + \mathrm{i}y^{\mathrm{T}}(\hat{q} - \bar{q}) \tag{C.3}$$

with parametric dependence on $\bar{q}$, also through $w(\bar{q})$ and $B(\bar{q})$, and on y. This Hamiltonian is put in normal form by the linear canonical transformation

$$(\hat{p}, \hat{q}) \longrightarrow (A^{-1}U^{\mathrm{T}}\hat{p}, AU^{\mathrm{T}}\hat{q}) \tag{C.4}$$

where the orthogonal matrix $U(\bar{q}) \equiv \{U_{k\mu}(\bar{q})\}$ diagonalizes the real symmetric matrix AB^2A as in equation (3.7). Let us also transform $y \longrightarrow A^{-1}U^{\mathrm{T}}y$ and $\bar{q} \longrightarrow AU^{\mathrm{T}}\bar{q}$, so that $\int \mathrm{d}y \longrightarrow (\det A)^{-1} \int \mathrm{d}y$ and

$$\hat{\mathcal{H}}_1 = w + \tfrac{1}{2}\sum\nolimits_k \left[\hat{p}_k^2 + \omega_k^2(\hat{q}_k - \bar{q}_k + \mathrm{i}\omega_k^{-2}y_k)^2 + \omega_k^{-2}y_k^2\right]. \tag{C.5}$$

Now we rescale the variables $y_k \to \omega_k^2 y_k$ and replace the known result (A.1) for the harmonic oscillator path integral, so that

$$\tilde{\rho}_0(q'', q'; \bar{q}) = \frac{\mathrm{e}^{-\beta w}}{\det A} \prod_k \frac{\beta\omega_k^2}{2\pi} \int \mathrm{d}y_k\ \mathrm{e}^{-\frac{1}{2}\beta\omega_k^2 y_k^2}\ \rho^{(\mathrm{h})}(q_k'' - \bar{q}_k + \mathrm{i}y_k, q_k' - \bar{q}_k + \mathrm{i}y_k; \omega_k)$$
$$= \frac{\mathrm{e}^{-\beta w}}{\det A} \prod_k \frac{1}{\sqrt{2\pi\beta}} \frac{f_k}{\sinh f_k} \frac{1}{\sqrt{2\pi\alpha_k}}$$
$$\times \exp\left(-\frac{\xi_k^2}{2\alpha_k} - \frac{\omega_k \coth f_k}{4}(q_k'' - q_k')^2\right) \tag{C.6}$$

where $\xi_k = (q_k'' + q_k')/2 - \bar{q}_k$ $f_k = \beta\omega_k/2$ and α_k is given by equation (3.9). In this equation the coordinate transformation (C.4) is to be understood also for the arguments of $\tilde{\rho}_0$, otherwise two further factors $\det A$ would appear, due to the transformation property of the path integral under (C.4) and to the definition (3.4) of $\tilde{\rho}$ under the analogous transformation for $\bar{q}$. For $q' = q'' = q$, $\tilde{\rho}_0(q, q; \bar{q})$ defines a Gaussian distribution in configuration space, centred at $\bar{q}$. The normalization constant is

$$\rho_{\mathrm{eff}}(\bar{q}) = \int \mathrm{d}q\ \tilde{\rho}_0(q, q; \bar{q}) = \frac{\mathrm{e}^{-\beta w(\bar{q})}}{(2\pi\beta)^{M/2}\det A} \prod_k \frac{f_k(\bar{q})}{\sinh f_k(\bar{q})} \equiv \frac{\mathrm{e}^{-\beta V_{\mathrm{eff}}(\bar{q})}}{(2\pi\beta)^{M/2}\det A} \tag{C.7}$$

and the second equality defines the effective potential V_{eff} as in the first equality of equation (3.13). The multidimensional Gaussian average $\langle\!\langle \cdots \rangle\!\rangle$ defined by $\tilde{\rho}_0$ is such that $\langle\!\langle (q_k - \bar{q}_k)(q_{k'} - \bar{q}_{k'}) \rangle\!\rangle \equiv \langle\!\langle \xi_k \xi_{k'} \rangle\!\rangle = \delta_{kk'}\alpha_k(\bar{q})$ which is indeed equivalent to equations (3.8) and (3.9).

Replacing the result for $\tilde{\rho}_0$ in equation (3.5) the average of an observable $\mathcal{O}(\hat{q})$ becomes

$$\mathcal{Z}_0\langle\mathcal{O}(\hat{q})\rangle_0 = \frac{(2\pi\beta)^{-M/2}}{\det A} \int \mathrm{d}q\ \mathcal{O}(q) \int \mathrm{d}\bar{q}\ \rho_0(q, q; \bar{q})$$
$$= \frac{(2\pi\beta)^{-M/2}}{\det A} \int \mathrm{d}\bar{q}\ \mathrm{e}^{-\beta V_{\mathrm{eff}}(\bar{q})} \int \mathrm{d}\xi\ \mathcal{O}(\bar{q} + \xi) \prod_k \frac{\mathrm{e}^{-\xi_k^2/2\alpha_k}}{\sqrt{2\pi\alpha_k}} \tag{C.8}$$

which coincides with equation (3.12).

Let us now derive expression (3.17) for the effective potential. Using equations (3.14) and (3.15) we have

$$\sum_k \omega_k^2(\bar{q})\,\alpha_k(\bar{q}) = \sum_k (UAB^2AU^{\mathrm{T}})_{kk}\,\alpha_k(\bar{q}) = \sum_{\mu\nu} B_{\mu\nu}^2(\bar{q}) D_{\mu\nu}(\bar{q})$$
$$= \sum_{\mu\nu} D_{\mu\nu}(\bar{q})\,\partial_{q_\mu}\partial_{q_\nu}\langle\!\langle V(\bar{q}+\xi)\rangle\!\rangle = 2\,\Delta(q)\,\mathrm{e}^{\Delta(q)}\,V(\bar{q}). \tag{C.9}$$

Then it is sufficient to use equations (3.10) and (3.16), and eventually to replace into the expression (3.13) of the effective potential.

The Weyl symbol for the PQSCHA density operator $\hat{\rho}_0$ follows from definition (3.24) in terms of its matrix elements $\rho_0(q'', q') = \int \mathrm{d}\bar{q}\,\tilde{\rho}_0(q'', q'; \bar{q})$ as obtained from (C.6):

$$\rho_0(p, q) = \left(\frac{2\pi}{\beta}\right)^{M/2} \frac{1}{\det A} \int \mathrm{d}\bar{q}\; \mathrm{e}^{-\beta V_{\mathrm{eff}}(\bar{q})} \prod_k \frac{\mathrm{e}^{-(q_k-\bar{q}_k)^2/2\alpha_k}}{\sqrt{2\pi\alpha_k}} \frac{\mathrm{e}^{-p_k^2/2\lambda_k}}{\sqrt{2\pi\lambda_k}} \tag{C.10}$$

where $\lambda_k(\bar{q}) = \omega_k(\bar{q})\coth f_k(\bar{q})/2$ are the quantum square fluctuations of the momenta in k-space. Replacing in equation (3.28), the PQSCHA expression (3.29) for the average of a general observable is obtained.

Appendix D. Standard PQSCHA: low-coupling approximation

In the LCA the renormalization parameters are expanded around the self-consistent minimum q_0 of $V_{\mathrm{eff}}(q)$. The Gaussian average defined by (3.8) and (3.9) can be correspondingly split, after equations (3.18), as $\langle\!\langle \cdots \rangle\!\rangle = \langle\!\langle \cdots \rangle\!\rangle_0 + \delta\langle\!\langle \cdots \rangle\!\rangle$, where $\langle\!\langle \cdots \rangle\!\rangle_0$ is calculated with the parameters $\alpha_k = \alpha_k(q_0)$ (i.e. $\omega_k = \omega_k(q_0)$ and, of course, $U = U(q_0)$). In order to keep control over the expansion of the effective potential we devise two dimensionless formal expansion labels

$$\alpha \sim \alpha_k \qquad \varepsilon \sim \alpha_k\big[\omega_k^2(q) - \omega_k^2\big]/\omega_k^2. \tag{D.1}$$

Note that $\alpha \sim \hbar$ and $\varepsilon \sim \hbar T$ at low temperature, whereas at high temperature $\alpha \sim \hbar^2/T$ and $\varepsilon \sim \hbar^2$. Then, the 'quantity'

$$\delta\Delta = \Delta(q) - \Delta = \tfrac{1}{2}\textstyle\sum_{\mu\nu}\big[D_{\mu\nu}(q) - D_{\mu\nu}\big]\partial_{q_\mu}\partial_{q_\nu} \;\sim\; \alpha\varepsilon \tag{D.2}$$

where $\Delta \equiv \Delta(q_0)$. The expansion of the logarithmic term of $V_{\mathrm{eff}}(\bar{q})$ gives

$$\frac{1}{\beta}\sum_k \ln\frac{\sinh f_k(q)}{f_k(q)} = \frac{1}{\beta}\sum_k \ln\frac{\sinh f_k}{f_k} + \Delta\left[\mathrm{e}^{\Delta(q)}V(q) - \mathrm{e}^{\Delta}V(q_0)\right] + \mathrm{O}(\alpha\varepsilon^2). \tag{D.3}$$

With this substitution, the effective potential (3.17) becomes

$$V_{\mathrm{eff}}(q) = (1-\delta\Delta)\,\mathrm{e}^{\delta\Delta}\,\mathrm{e}^{\Delta}\;V(q) - \Delta\mathrm{e}^{\Delta}\;V(q_0) + \frac{1}{\beta}\sum_k \ln\frac{\sinh f_k}{f_k} + \mathrm{O}(\alpha\varepsilon^2)$$
$$= \mathrm{e}^{\Delta}\;V(q) - \Delta\mathrm{e}^{\Delta}\;V(q_0) + \frac{1}{\beta}\sum_k \ln\frac{\sinh f_k}{f_k} + \mathrm{O}(\alpha\varepsilon^2) \tag{D.4}$$

which is equation (3.19). Indeed, the neglected terms in $(\delta\Delta)^2$ are of order $\alpha^2\varepsilon^2$.

Appendix E. Nonstandard system: path integral

In this appendix we show how to get the path integral (5.1) for the density matrix in the coordinate representation, $\rho(q'', q')$, starting from the result given in equation (1.9) of [105]. Replacing $t_1 = 0$ and $it_2 = \beta$, we have for its Weyl symbol

$$\rho(p,q) = \int \mathcal{D}[p] \int \mathcal{D}[q] \exp\left\{ \int_0^\beta \mathrm{d}u \left[\frac{\mathrm{i}}{2}\left(p^{\mathrm{T}}(u)\dot{q}(u) - \dot{p}^{\mathrm{T}}(u)q(u)\right) - \mathcal{H}\left(p(u), q(u)\right)\right] \right.$$
$$-\mathrm{i}\left[p - \frac{p(\beta)+p(0)}{4}\right]^{\mathrm{T}}\left[q(\beta)-q(0)\right]$$
$$\left. +\mathrm{i}\left[q - \frac{q(\beta)+q(0)}{4}\right]^{\mathrm{T}}\left[p(\beta)-p(0)\right]\right\}. \tag{E.1}$$

In this expression, we can perform the integration by parts

$$\int_0^\beta \mathrm{d}u\, \dot{p}^{\mathrm{T}}(u)\, q(u) = p^{\mathrm{T}}(\beta)\, q(\beta) - p^{\mathrm{T}}(0)\, q(0) - \int_0^\beta \mathrm{d}u\, p^{\mathrm{T}}(u)\, \dot{q}(u) \tag{E.2}$$

getting

$$\rho(p,q) = \int \mathcal{D}[p] \int \mathcal{D}[q] \exp\left\{ \int_0^\beta \mathrm{d}u \left[\mathrm{i}p^{\mathrm{T}}(u)\dot{q}(u) - \mathcal{H}\left(p(u), q(u)\right)\right] \right.$$
$$\left. -\mathrm{i}p^{\mathrm{T}}\left[q(\beta)-q(0)\right] + \mathrm{i}\left[q - \frac{q(\beta)+q(0)}{2}\right]^{\mathrm{T}}\left[p(\beta)-p(0)\right]\right\}. \tag{E.3}$$

Note that the integral over $p(\beta)$ can be extracted from the path integral and performed, resulting in the boundary condition $\frac{1}{2}[q(0)+q(\beta)] = q$. Using equation (3.26) we eventually get the path integral (5.1) with the action (5.2).

Appendix F. Nonstandard PQSCHA

In this appendix we evaluate the expression for $\bar{\rho}_0(q'', q'; \bar{p}, \bar{q})$, namely equation (5.5) with the action S_0 given by (5.2) with $\mathcal{H}$ replaced by $\mathcal{H}_0$, equation (5.6). We rewrite $\bar{\rho}_0$ as

$$\bar{\rho}_0(q'', q'; \bar{p}, \bar{q}) = \left(\frac{\beta}{2\pi}\right)^{2M} \int \mathrm{d}z\, \mathrm{d}y \int \mathcal{D}[p] \int_{q'}^{q''} \mathcal{D}[q]$$
$$\times \exp\left(S_0[p,q] + \mathrm{i}\int_0^\beta \mathrm{d}u \left[z^{\mathrm{T}}\left(\bar{p} - p(u)\right) + y^{\mathrm{T}}\left(\bar{q} - q(u)\right)\right]\right)$$
$$\equiv \left(\frac{\beta}{2\pi}\right)^{2M} \int \mathrm{d}z\, \mathrm{d}y\ \rho_1(q'', q'; \bar{p}, \bar{q}; y, z). \tag{F.1}$$

The auxiliary phase-space integration variables (y, z) arise from the Fourier representation of the delta functions. In this way $(\bar{p}, \bar{q})$ appear in the path integral only as parameters, and $\rho_1(q'', q'; \bar{p}, \bar{q}; y, z)$ is the density matrix corresponding to the quadratic Hamiltonian function

$$\mathcal{H}_1 = w + \tfrac{1}{2}\delta p^{\mathrm{T}}\, \boldsymbol{A}^2\, \delta p + \delta p^{\mathrm{T}}\, \boldsymbol{X}\, \delta q + \tfrac{1}{2}\delta q^{\mathrm{T}}\, \boldsymbol{B}^2\, \delta q + z^{\mathrm{T}}\, \delta p + y^{\mathrm{T}}\, \delta q \tag{F.2}$$

where $(\delta p, \delta q) = (p - \bar{p}, q - \bar{q})$. Now, using equations (5.7) and (5.9), and the canonical transformation (5.8) for all phase-space variables, we find the normal form of $\mathcal{H}_1$:

$$\mathcal{H}_1 = w + \sum_k \left[\tfrac{1}{2}\,\delta p_k^2 + \sigma_k\, \delta p_k\, \delta q_k + \tfrac{1}{2}(\omega_k^2 + \sigma_k^2)\, \delta {q_k}^2 + z_k\, \delta p_k + y_k\, \delta {q_k}^2\right]$$

$$= w + \tfrac{1}{2}\sum_k \left[\widetilde{p}_k^2 + \omega_k^2 \widetilde{q}_k^2 + z_k^2 + \widetilde{y}_k^2\right] \tag{F.3}$$

where $(\widetilde{p}_k, \widetilde{q}_k) = (p_k - \bar{p}_k + \sigma_k \bar{q}_k + \mathrm{i}z_k,\ q_k - \bar{q}_k + \mathrm{i}\widetilde{y}_k)$ and $\widetilde{y}_k = (y_k - \sigma_k z_k)/\omega_k^2$. For the first term in the action we have

$$\int_0^\beta \mathrm{d}u\, \boldsymbol{p}^{\mathrm{T}} \dot{\boldsymbol{q}} = \sum_k \left\{ (\bar{p}_k + \sigma_k \bar{q}_k - \mathrm{i}z_k)\left[q_k(\beta) - q_k(0)\right] \right.$$
$$\left. -\frac{\sigma_k}{2}\left[q_k^2(\beta) - q_k^2(0)\right] + \int_0^\beta \mathrm{d}u\, \widetilde{p}_k \dot{\widetilde{q}}_k \right\}$$

so we are reduced to the harmonic oscillator path integral and

$$\rho_1(q'', q'; \bar{p}, \bar{q}; y, z) = \mathrm{e}^{-\beta w} \prod_k \rho^{(\mathrm{h})}(q_k'' - \bar{q}_k + \widetilde{y}_k, q_k' - \bar{q}_k + \widetilde{y}_k; \omega_k)$$
$$\times \prod_k \exp\left[-\frac{\beta}{2}\left(z_k^2 + \widetilde{y}_k^2\right) + \mathrm{i}(\bar{p}_k + \sigma_k \bar{q}_k - z_k)(q_k'' - q_k') - \mathrm{i}\frac{\sigma_k}{2}\left(q_k''^2 - q_k'^2\right)\right] \tag{F.4}$$

in terms of the harmonic density matrix (A.1) Now we can replace ρ_1 in equation (F.1) and do the Gaussian quadratures, eventually getting

$$\bar{\rho}_0(q'', q'; \bar{p}, \bar{q}) = \frac{\mathrm{e}^{-\beta w}}{(2\pi)^M} \prod_k \frac{f_k}{\sinh f_k} \mathrm{e}^{\mathrm{i}(\bar{p}_k - \sigma_k \xi_k)\zeta_k} \sqrt{\frac{\omega_k}{\pi \mathcal{L}_k}} \exp\left(-\frac{\omega_k}{\mathcal{L}_k}\xi_k^2 - \frac{\omega_k \mathcal{L}_k}{4}\zeta_k^2\right)$$

where $\mathcal{L}_k = \coth f_k - f_k^{-1}$, $f_k = \beta\omega_k/2$, $\xi_k = (q_k'' + q_k')/2 - \bar{q}_k$ and $\zeta_k = q_k'' - q_k'$. Using equation (3.24) the corresponding Weyl symbol is obtained,

$$\bar{\rho}_0(p, q; \bar{p}, \bar{q}) = \mathrm{e}^{-\beta w} \prod_k \frac{f_k}{\sinh f_k} \frac{1}{\pi \mathcal{L}_k} \exp\left[-\frac{\omega_k}{\mathcal{L}_k}\xi_k^2 - \frac{1}{\omega_k \mathcal{L}_k}(\eta_k + \sigma_k \xi_k)^2\right] \tag{F.5}$$

with, now, $(\eta_k, \xi_k) = (p_k - \bar{p}_k, q_k - \bar{q}_k)$. This is a Gaussian distribution in phase space, centred in $(\bar{p}, \bar{q})$, with normalization constant

$$\int \mathrm{d}p\, \mathrm{d}q\ \bar{\rho}_0(p, q; \bar{p}, \bar{q}) = \mathrm{e}^{-\beta w(\bar{p}, \bar{q})} \prod_k \frac{f_k(\bar{p}, \bar{q})}{\sinh f_k(\bar{p}, \bar{q})} \equiv \mathrm{e}^{-\beta \mathcal{H}_{\mathrm{eff}}(\bar{p}, \bar{q})} \tag{F.6}$$

giving the identification (5.17) of the effective Hamiltonian $\mathcal{H}_{\mathrm{eff}}$, and the $\bar{\rho}_0$ averages $\langle\!\langle \cdots \rangle\!\rangle$ are such that

$$\left\langle\!\left\langle \xi_k^2 \right\rangle\!\right\rangle = \frac{\mathcal{L}_k}{2\omega_k} \qquad \left\langle\!\left\langle \xi_k(\eta_k + \sigma_k \xi_k) \right\rangle\!\right\rangle = 0 \qquad \left\langle\!\left\langle (\eta_k + \sigma_k \xi_k)^2 \right\rangle\!\right\rangle = \frac{\omega_k \mathcal{L}_k}{2}. \tag{F.7}$$

These equations are equivalent to (5.11).

References

[1] Feynman R P and Hibbs A R 1965 *Quantum Mechanics and Path Integrals* (New York: McGraw Hill)
[2] Feynman R P 1972 *Statistical Mechanics* (Reading, MA: Benjamin)
[3] Giachetti R and Tognetti V 1985 *Phys. Rev. Lett.* **55** 912
[4] Giachetti R and Tognetti V 1986 *Phys. Rev.* B **33** 7647
[5] Feynman R P and Kleinert H 1986 *Phys. Rev.* A **34** 5080
[6] Cuccoli A, Tognetti V and Vaia R 1991 *Phys. Rev.* A **44** 2734
[7] Cuccoli A, Tognetti V, Verrucchi P and Vaia R 1992 *Phys. Rev.* A **45** 8418
[8] Kleinert H 1990 *Path Integrals in Quantum Mechanics, Statistics and Polymer Physics* (Singapore: World Scientific)
[9] Weiss U 1993 *Quantum Dissipation* (Singapore: World Scientific)
[10] Cuccoli A, Livi R, Spicci M, Tognetti V and Vaia R 1994 *Int. J. Mod. Phys.* B **8** 2391

[11] Cowley E R and Horton G K 1995 *Dynamic Properties of Solids* vol 7, ed G K Horton and A A Maradudin (Amsterdam: North-Holland)
[12] Voth G A 1996 *Adv. Chem. Phys.* at press
[13] Wigner E P 1932 *Phys. Rev.* **40** 749
[14] Hillery M, O'Connell R F, Scully M O and Wigner E P 1984 *Phys. Rep.* **106** 122
[15] Kirkwood J G 1933 *Phys. Rev.* **44** 31
[16] Imre K, Ozizmir E, Rosenbaum M and Zweifel P 1967 *J. Math. Phys.* **8** 1097
[17] Fujiwara Y, Osborn T A and Wilk S F J 1982 *Phys. Rev.* A **25** 14
[18] Weyl H 1950 *The Theory of Groups and Quantum Mechanics* (New York: Dover)
[19] Glauber R J 1963 *Phys. Rev.* **131** 2766
[20] Louisell W H 1973 *Quantum Statistical Properties of Radiation* (New York: Wiley)
[21] Klauder J R 1985 *Coherent States* (Singapore: World Scientific)
[22] Peierls R 1938 *Phys. Rev.* **54** 918
[23] Buettner H and Flytzanis N 1987 *Phys. Rev.* A **36** 3443
[24] Kampf A and Schön G 1987 *Phys. Rev.* B **36** 3651
[25] Kleinert H 1986 *Phys. Lett.* **118A** 195
[26] Kleinert H 1986 *Phys. Lett.* **118A** 267
[27] Kleinert H 1986 *Phys. Lett.* **181B** 324
[28] Janke W and Kleinert H 1986 *Phys. Lett.* **118A** 371
[29] Janke W and Kleinert H 1987 *Chem. Phys. Lett.* **137** 162
[30] Janke W 1989 *Path Integrals from meV to MeV* ed V Sa-yakanit *et al* (Singapore: World Scientific) p 355
[31] Srivastava S and Vishwamittar V 1991 *Phys. Rev.* A **44** 8006
[32] Kleinert H 1992 *Phys. Lett.* **280B** 251
[33] Kleinert H 1993 *Phys. Lett.* **173A** 1332
[34] Messina M, Schenter G K and Garrett B C 1993 *J. Chem. Phys.* **98** 4120
[35] Kleinert H and Meyer H 1994 *Phys. Lett.* **184A** 319
[36] Vaia R and Tognetti V 1990 *Int. J. Mod. Phys.* B **4** 2005
[37] Voth G A, Chandler D and Miller W H 1989 *J. Chem. Phys* **91** 7749
[38] Messina M, Schenter G K and Garrett B C 1993 *J. Chem. Phys.* **98** 8525
[39] Voth G A 1993 *J. Phys. Chem.* **97** 8365
[40] Giachetti R and Tognetti V 1986 *J. Magn. Magn. Mater.* **54–57** 861
[41] Giachetti R and Tognetti V 1987 *Phys. Rev.* B **36** 5512
[42] Giachetti R, Tognetti V and Vaia R 1988 *J. Physique Coll.* C8 **49** 1589
[43] Giachetti R, Tognetti V and Vaia R 1988 *Phys. Rev.* A **37** 2165
[44] Giachetti R, Tognetti V and Vaia R 1988 *Phys. Rev.* A **38** 1521
[45] Giachetti R, Tognetti V and Vaia R 1988 *Phys. Rev.* A **38** 1638
[46] Cuccoli A, Spicci M, Tognetti V and Vaia R 1992 *Phys. Rev.* B **45** 10 127
[47] Völkel A R, Cuccoli A, Spicci M and Tognetti V 1993 *Phys. Lett.* **182A** 60
[48] Cuccoli A, Tognetti V and Vaia R 1990 *Phys. Rev.* B **41** 9588
[49] Liu S, Horton G K and Cowley E R 1991 *Phys. Lett.* **152A** 79
[50] Liu S, Horton G K and Cowley E R 1991 *Phys. Rev.* B **44** 11 714
[51] Liu S, Horton G K, Cowley E R, McGurn A R, Maradudin A A and Wallis R F 1992 *Phys. Rev.* B **45** 9716
[52] Zhu Z, Liu S, Horton G K and Cowley E R 1992 *Phys. Rev.* B **45** 7122
[53] Cuccoli A, Macchi A, Neumann M, Tognetti V and Vaia R 1992 *Phys. Rev.* B **45** 2088
[54] Cuccoli A, Macchi A, Tognetti V and Vaia R 1993 *Phys. Rev.* B **47** 14 923
[55] Cowley E R, Freidkin E and Horton G K 1994 *Ferroelectrics* **153** 43
[56] Acocella D, Horton G K and Cowley E R 1995 *Phys. Rev.* B **51** 11 406
[57] Okopinska A 1987 *Phys. Rev.* D **35** 1835
[58] Vlachos K and Okopinska A 1994 *Phys. Lett.* **186A** 375
[59] Acocella D, Horton G K and Cowley E R 1995 *Phys. Rev. Lett.* **74** 4887
[60] Voth G A 1991 *J. Chem. Phys.* **94** 4095
[61] Cao J and Voth G A 1994 *J. Chem. Phys.* **100** 5093
[62] Giachetti R, Tognetti V and Vaia R 1988 *Path Summation: Achievements and Goals* ed S Lundqvist, A Ranfagni, V Sa-yakanit and L S Schulman (Singapore: World Scientific) p 92
[63] Giachetti R, Tognetti V and Vaia R 1990 *Applications of Statistical and Field Theory Methods to Condensed Matter* ed D Baeriswyl, A R Bishop and J Carmelo (New York: Plenum Press) p 141
[64] Doll J D, Coalson R D and Freeman D L 1985 *Phys. Rev. Lett.* **55** 1
[65] Lobaugh J and Voth G A 1992 *J. Chem. Phys.* **97** 4205

[66] Wouters S and De Raedt H 1987 *Magnetic Excitations and Fluctuations II* ed U Balucani, S W Lovesey, M G Rasetti and V Tognetti (Berlin: Springer) p 204
[67] Cuccoli A, Macchi A, Tognetti V, Pedrolli G and Vaia R 1995 *Phys. Rev.* B **51** 12369
[68] Leschke H 1988 *Path Summation: Achievements and Goals* ed S Lundqvist, A Ranfagni, V Sa-yakanit and L S Schulman (Singapore: World Scientific) p 399
[69] Cuccoli A, Tognetti V, Verrucchi P and Vaia R 1993 *Path Integrals from meV to MeV: Tutzing 1992* ed A Inomata and U Weiss (Singapore: World Scientific) p 244
[70] Cuccoli A, Tognetti V, Verrucchi P and Vaia R 1993 *Path Integrals in Physics* ed V Sa-yakanit *et al* (Singapore: World Scientific)
[71] Cuccoli A, Tognetti V, Verrucchi P and Vaia R 1991 *Phys. Rev.* B **44** 903
[72] Cuccoli A, Tognetti V, Verrucchi P and Vaia R 1992 *Phys. Rev.* B **46** 11601
[73] Cuccoli A, Tognetti V, Verrucchi P and Vaia R 1993 *J. Appl. Phys.* **73** 6998
[74] Cuccoli A, Tognetti V, Verrucchi P and Vaia R 1994 *J. Appl. Phys.* **75** 5814
[75] Cuccoli A, Tognetti V, Verrucchi P and Vaia R 1995 *J. Magn. Magn. Mater.* **140–144** 1703
[76] Cuccoli A, Tognetti V, Verrucchi P and Vaia R 1995 *Phys. Rev.* B **51** 12840
[77] Cuccoli A, Tognetti V and Vaia R 1991 *Phys. Lett.* **160A** 184
[78] Cuccoli A, Maradudin A A, McGurn A R, Tognetti V and Vaia R 1992 *Phys. Rev.* B **46** 8839
[79] Macchi A, Maradudin A A and Tognetti V (1995) *Phys. Rev.* B **52** 241
[80] Cuccoli A, Maradudin A A, McGurn A R, Tognetti V and Vaia R 1993 *Phys. Rev.* B **48** 7015
[81] Cuccoli A, Spicci M, Tognetti V and Vaia R 1993 *Phys. Rev* B **47** 7859
[82] Cuccoli A, Tognetti V, Maradudin A A, McGurn A R and Vaia R 1994 *Phys. Lett.* **196A** 285
[83] Mori H 1965 *Prog. Theor. Phys.* **33** 423
[84] Mori H 1965 *Prog. Theor. Phys.* **34** 399
[85] Dupuis M 1967 *Prog. Theor. Phys.* **37** 502
[86] Cao J and Voth G A 1993 *J. Chem. Phys.* **99** 10070
[87] Thirumalai D and Berne B J 1983 *J. Chem. Phys.* **79** 5029
[88] Cao J and Voth G A 1994 *J. Chem. Phys.* **100** 5106
[89] Cao J and Voth G A 1994 *J. Chem. Phys.* **101** 6157
[90] Schenter G K, Messina M and Garrett B C 1993 *J. Chem. Phys.* **99** 1674
[91] Cao J and Voth G A 1994 *J. Chem. Phys.* **101** 6168
[92] Born M and von Kármán T 1912 *Z. Phys.* **13** 297
[93] Maradudin A A, Montroll E W and Weiss G H 1963 *Theory of Lattice Dynamics in the Harmonic Approximation Solid State Physics—Supplement 3* (London: Academic)
[94] Hooton D J 1955 *Phil. Mag.* **46** 422
[95] Koehler T R 1966 *Phys. Rev. Lett.* **17** 89
[96] Horton G K, Klein M L and Goldaman V V 1969 *J. Low. Temp. Phys.* **1** 391
[97] Horton G K 1976 *Rare Gas Solids* ed M L Klein and J A Venables (London: Academic) p 1
[98] Jensen J L W V 1906 *Acta. Math.* **30** 175
[99] Kleinert H 1986 *Phys. Lett.* **118A** 267
[100] Janke W and Cheng B K 1988 *Phys Lett.* **129A** 140
[101] Cowley E R and Horton G K 1992 *Ferroelectrics* **136** 157
[102] Pollock E L and Ceperley D M 1984 *Phys. Rev.* B **30** 2555
[103] Neumann M and Zoppi M 1989 *Phys. Rev.* A **40** 4572
[104] Poll J D and Miller M S 1971 *J. Chem. Phys.* **54** 2673
[105] Berezin F A 1980 *Sov. Phys.–Usp.* **23** 763
[106] Giachetti R, Tognetti V and Vaia R 1989 *Phys. Scr.* **40** 451
[107] Giachetti R, Tognetti V and Vaia R 1989 *J. Physique Coll.* C3 59
[108] Schneider T and Stoll E 1980 *Phys. Rev.* B **22** 5317
[109] Janke W and Sauer T 1995 *Phys. Lett.* **197A** 335
[110] Moraldi M, Pini M G and Rettori A 1984 *Phys. Rev.* A **31** 1971
[111] Dashen R F, Hasslacher B and Neveu A 1974 *Phys. Rev.* D **10** 4144
[112] Maki K and Takayama H 1979 *Phys. Rev.* B **20** 3223 and 5009
[113] Maki K and Takayama H 1979 *Phys. Rev.* B **20** 3223
[114] Fowler M and Zotos X 1986 *Phys. Rev.* B **25** 5806
[115] Gürsey F 1950 *Proc. Camb. Phil. Soc.* **46** 182
[116] Hénon M 1974 *Phys. Rev.* B **9** 1921
[117] Flaschka H 1974 *Phys. Rev.* B **9** 1924
[118] Kac M and Moerbeke P V 1975 *Proc. Natl Acad. Sci. USA* **72** 1627, 2879

[119] Olshanetsky M A and Perelomov A M 1977 *Lett. Math. Phys.* **2** 7
[120] Toda M and Saitoh N 1983 *J. Phys. Soc. Japan* **52** 3703
[121] Mertens F G 1984 *Z. Phys.* B **55** 353
[122] Hader M and Mertens F G 1985 *Phys. Lett.* **112A** 309
[123] Hader M and Mertens F G 1986 *J. Phys. A: Math. Gen.* **19** 1913
[124] Hader M and Mertens F G 1987 *Z. Phys.* **69** 121
[125] Gruner-Bauer P and Mertens F G 1988 *Z. Phys.* B **70** 435
[126] McGurn A R, Ryan P, Maradudin A A and Wallis R F 1989 *Phys. Rev.* B **40** 2407
[127] Horton G K and Cowley E R 1994 *Die Kunst of Phonons* ed T Paszkiewicz and R Rapcewicz (New York: Plenum) p 1
[128] Peterson O G, Batchelder D N and Simmons R O 1966 *Phys. Rev.* **150** 703
[129] Peek D A, Fujita I, Schmidt M C and Simmons R O 1992 *Phys. Rev.* B **45** 9680
[130] Fradkin M A, Zheng S X and Simmons R O 1994 *Phys. Rev.* B **49** 3197
[131] Arnold V I 1975 *Mathematical Methods of Classical Mechanics* (Moscow: Mir)
[132] Leschke H and Wonneberger S 1989 *Path Integrals from meV to MeV* ed V Sa-yakanit *et al* (Singapore: World Scientific) p 480
[133] Villain J 1974 *J. Physique* **35** 27
[134] Blume M, Heller P and Lurie N A 1975 *Phys. Rev.* B **11** 4483
[135] Ramirez A P and Wolf W P 1985 *Phys. Rev.* B **32** 1639
[136] Steiner M, Kakurai K and Kjems J K 1983 *Z. Phys.* B **53** 117
[137] Cuccoli A, Tognetti V and Vaia R 1995 *Phys. Rev.* B **52** at press
[138] Ding H Q 1992 *Phys. Rev.* B **45** 230
[139] Its A R, Izergin A G, Korepin V E and Slavnov N A 1993 *Phys. Rev. Lett.* **70** 1704
[140] Kubo R 1966 *Rep. Prog. Phys.* **29** 255
[141] Zwanzig R 1965 *Annual Review of Physical Chemistry* vol 16, ed H Eyring (Palo Alto, CA: Annual Reviews Inc.)
[142] Tomita H and Mashiyama H 1972 *Prog. Theor. Phys.* **48** 1133
[143] Balucani U and Tognetti V 1977 *Phys. Rev.* B **16** 271
[144] Lee M H, Hong J and Florencio J Jr 1987 *Phys. Scr.* T **19** 498
[145] Berne B J and Pecora R 1976 *Dynamic Light Scattering* (London: Wiley)
[146] De Raedt H and De Raedt B 1977 *Phys. Rev.* B **15** 5357
[147] De Raedt H and De Raedt B 1978 *Phys. Rev.* B **18** 2039
[148] Visvanath V S and Müller G 1990 *J. Appl. Phys.* **67** 5486
[149] Lovesey S W and Meserve R A 1972 *J. Phys. C: Soilid State Phys.* **6** 79
[150] Tomita K and Tomita H 1971 *Prog. Theor. Phys.* **45** 1407
[151] Kleinert H 1995 *Preprint*
[152] Ceperley D M 1995 *Rev. Mod. Phys.* **67** 279
[153] Müser M H, Nielaba P and Binder K 1995 *Phys. Rev.* B **51** 2723
[154] Schweizer K S, Stratt R M, Chandler D and Wolynes P G 1981 *J. Chem. Phys.* **75** 1347
[155] Takahashi M and Imada M 1984 *J. Phys. Soc. Japan* **53** 3765
[156] Friesner R A and Levy R M 1984 *J. Chem. Phys.* **80** 4488
[157] Freeman D L and Doll J D 1984 *J. Chem. Phys.* **80** 5709